Project Number: WMC 8008

Compressible Gas Flow Experiment and Assisted COMSOL Modeling

A Major Qualifying Project

Submitted to the Faculty

of the

WORCESTER POLYTECHNIC INSTITUTE

in partial fulfillment of the requirements for the

Degree of Bachelor of Science

By

_____

Jared Brown

_____

Michael Lynch

_____

Taylor Mazzali

_____

Ryan Vautrin

_____

Ross Yaylaian

Approved:

_____

Professor William M. Clark, Project Advisor

Abstract

The goal of this project was to construct a working compressible gas flow laboratory experiment for a Unit Operations class and to successfully model the experiment in COMSOL Multiphysics. We designed and constructed an experiment to measure pressure drops and friction factors for air flow in pipes, based on an article in *Chemical Engineering Education* by two Lehigh University professors. We developed a computer simulation to effectively model the process. Through experimentation it was found that increasing pressure in the pipe increased the density and, therefore, decreased the velocity of the fluid and the pressure drop along the pipe. The simulated values showed the same trends as the experimental ones, thus proving to be an effective educational tool for demonstrating the concept of pressure drop across a length of pipe.

Acknowledgements

We would first like to thank our advisor, Professor William M. Clark for his help and guidance throughout the project. His input and supervision on the construction of the apparatus was vital, as well as his advice for the COMSOL model.

Secondly, we would like to thank Mr. Jack Ferraro for his assistance in ordering the parts required for our apparatus and also with his assistance in constructing the apparatus.

Table of Contents

Table of Figures

Table of Tables

Introduction

Compressible flow is an important concept in the field of Chemical Engineering, yet at Worcester Polytechnic Institute it is an under-examined topic in the curriculum on the way to obtaining a degree. Understanding this, our MQP group and Professor Clark decided to create a Unit Operations laboratory experiment for seniors in the Chemical Engineering field. Basing our experiment off of an article that was found in *Chemical Engineering Education [1];* our group designed our apparatus and ordered our parts as well as modeled the experiment in COMSOL Multiphysics to get a fully functioning simulation.

In the chemical engineering sequence senior year at Worcester Polytechnic Institute students are given the opportunity to apply their knowledge obtained from the classroom to real world situations and applications. Two unit operations courses introduce experiments focused on laboratory practice to help enforce the culmination of their studies throughout their undergraduate years. Proper laboratory procedure and safety is taught using many different types of apparatuses that can be found throughout the chemical engineering field. These projects also foster the development of proper group dynamics and collaboration, which are necessary to complete their tasks within the given deadlines.

Though these experiments focus on a wide variety of subjects, the topic of compressible flow and its effects on pressure drop appear to be lacking. Compressible flow has often been an undereducated aspect of chemical engineering, but is important to many different careers in which piping systems are used. Changes in piping pressure, flow rate, gas density and velocity all effect the pressure drop across the pipe and without careful consideration can cause numerous complications and hazards in the work environment. The piping equipment constructed in Goddard Hall was constructed to enhance students' understanding of compressible flow by illustrating the effects that changing conditions have on the properties of compressible gas.

The utilization of the engineering software COMSOL can be used as a pre-laboratory instrument to give students a visual representation of how compressible a fluid will behave under different conditions in the piping, preparing them for the upcoming experiments. COMSOL can also be used as a basis of comparison to experimental results determined in the lab. Upon completion of the experiment and subsequent laboratory report, students should have a firm understanding of the concepts and difficulties associated with compressible flow.

Background and Theory

In the vast subjects of chemical engineering covered at Worcester Polytechnic Institute the study of compressible flow is often an overlooked field. Compressible flow can be found in a wide array of industries with piping systems. Essentially all chemical plants require the use of piping systems to transport necessary fluids to the process equipment. Fluids, both liquids and gases are mainly used in piping systems, but for the purposes of compressible flow, gas is its most common form.

Complications can arise when dealing with compressible fluids as compared to their incompressible counterparts. Changes in fluid properties such as density, pressure and temperature affect the pressure drop and volumetric flow rate along the pipe for compressed gases. Design specifications of equipment may be inadequate to handle flows without careful analysis of fluid properties. This can affect the overall system efficiency or in a worst case scenario cause malfunctions and failure in equipment. In cases where explosive gases are involved, extreme care must be taken to ensure a safe work environment. On the other hand, incompressible flow has none of these variables to consider. Usually incompressible fluids are in a liquid state and are therefore very difficult to compact any further.

Darcy-Weisbach Equation

Many of the changes in pressure drop across the piping can be associated with a few design variables. The most obvious specification is the length of the piping. The longer the piping length the greater the pressure drop at the end of the piping. This is due to the friction loss associated with the fluid running along the unsmooth piping [2].

Any pressure change in the fluid plays an important role in the flow and outlet pressure from the piping. As the pressure within the system is increased (keeping the mass flowrate constant) the gas is further compressed, resulting in a denser fluid. As the density of the fluid is increased this will result in a slower velocity, causing a lower pressure drop across the pipe. The opposite is also true; as pressure is decreased the fluid will become less dense, and the velocity and pressure drop will increase. These relationships can be expressed by the Darcy-Weisbach equation which can be seen below:

$$\Delta P = f(L/D)\rho\frac{V^2}{2} \qquad (1)$$

Where:

$\Delta P = \text{Pressure Drop}$(ft of water)
f = Darcy Friction factor (Dimensionless)
L = Length of pipe (ft)

D = Diameter of pipe (ft)
ρ = Density of fluid (lbs/ft^3)
V = Velocity (ft/s)

Reynolds Number

The Reynold's number is a dimensionless value that is used to determine the type of fluid flow within a pipe. Reynold's number is used in calculating the Darcy friction factor, which in turn determines pressure drop in the Darcy-Weisbach equation. With an increasing Reynold's number the pressure drop also increases while the friction factor decreases. Using the equation seen below, if the value is at or below 2,100 it is laminar indicating high viscous forces within the fluid. Turbulent flow is found to occur when values are above 4,000 when inertial forces are larger than viscous forces, forcing the Reynold's number up. In other words turbulence is agitation of the moving fluid, moving in many different directions, opposed to a smooth orderly one directional movement. Due to the nature of turbulent flow the pipe roughness affects the pressure drop causing a greater amount of friction that decreases the velocity of the gas. Additionally, temperature also plays a significant role in the determination of the flows characteristics. With a rise in temperature in the piping the viscosity of the fluid will diminish and can raise the Reynolds number further into the turbulent range.

$$Re = \frac{\rho VD}{\mu g_c} \qquad (2)$$

Where:

ρ is the density of the gas (lb_m/ft^3)
V is the velocity (ft/sec)
D is the diameter (ft)
μ is the dynamic viscosity (lb_f*s/ft^2)
g_c is the gravity constant (32.17 $lb_m ft/lb_f sec^2$)

Darcy Friction Factor

The Darcy friction factor is a dimensionless quantity that factors for friction losses as the fluid flows through a pipe. This factor relies on both the Reynolds number of the flow and the inside diameter of the pipe. The Darcy friction factor can be found graphically by using a Moody diagram. It can also be calculated using mathematical models, which are the Colebrook, Haaland, and Swamee-Jain equations.

Moody Diagram

The Moody diagram utilizes the Reynolds number of a flow, as well as the diameter and roughness of the pipe in order to find the Darcy friction factor. The diagram is constructed completely with dimensionless values, so no conversions are necessary to use it. An example of the Moody diagram can be seen in the following figure.

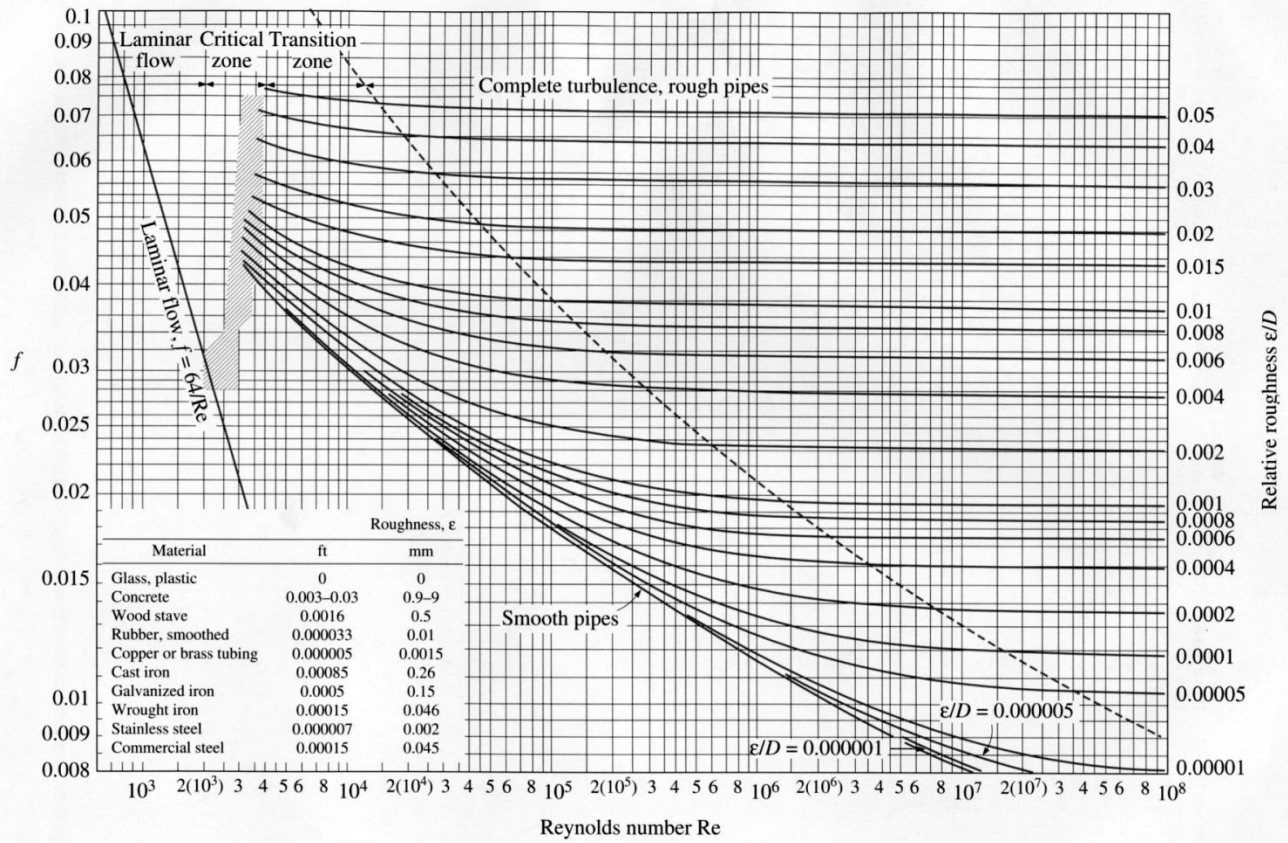

Figure 1: Moody Diagram [3]

Colebrook Equation

The Colebrook equation is a method used to solve for the Darcy friction factor iteratively, based on the diameter of the pipe and the Reynolds number of the flow. The Colebrook equation is as follows [2]:

$$\frac{1}{\sqrt{f}} = -2\log_{10}\left(\frac{\varepsilon/D_h}{3.7} + \frac{2.51}{Re\sqrt{f}}\right) \qquad (3)$$

Where:

- f is the Darcy friction factor (dimensionless)
- ε is the Roughness height of the pipe (ft)

- D_h is the hydraulic diameter of the pipe (ft)
- Re is the Reynolds number (dimensionless)

Haaland Equation

The Haaland equation is an approximation of the Colebrook method, which allows for the friction factor to be solved directly rather than with iterations. Even though it is only an approximation, the Haaland method returns values very similar to that of the Colebrook method. It is as follows [17]:

$$\frac{1}{\sqrt{f}} = -1.8\log_{10}\left[\left(\frac{\varepsilon/D}{3.7}\right)^{1.11} + \frac{6.9}{Re}\right] \qquad (4)$$

Where:

- f is the Darcy friction factor (dimensionless)
- ε is the Roughness height of the pipe (ft)
- D is the inside diameter of the pipe (ft)
- Re is the Reynolds number (dimensionless)

Swamee-Jain Equation

Like the Haaland method, the Swamee-Jain method of calculating the Darcy friction factor is an approximation of the Colebrook equation, which allows for the friction factor to be solved directly. Though it is less accurate than both the Colebrook and Haaland methods, the calculation is much simpler. The Swamee-Jain equation is as follows [18]:

$$f = \frac{0.25}{\left[\log_{10}\left(\frac{\varepsilon}{3.7D} + \frac{5.74}{Re^{0.9}}\right)\right]^2} \qquad (5)$$

Where:

- f is the Darcy friction factor (dimensionless)
- ε is the Roughness height of the pipe (ft)
- D_h is the hydraulic diameter of the pipe (ft)
- Re is the Reynolds number (dimensionless)

Methodology

There were two distinct parts to the methodology for this MQP. The first was the COMSOL modeling portion in which a model was created to test certain parameters of the system. The second part was using the actual physical apparatus to perform experiments and determine what students in a unit operations laboratory would do for this experiment.

COMSOL Modeling

The first portion of this project revolved around the creation and implementation of a COMSOL computer model of the system. With this model created, the team could experiment on the apparatus and the computer model and compare the results. The computer model should give ideal results since it is calculating with a completely smooth pipe, while the apparatus would give comparable data.

To begin, the COMSOL 3.5 program is only located on the Sunfire server; necessitating the use of the remote desktop program to access it. Once within the program, a model must be chosen from the many available options. The model chosen was the k-ε Turbulence Model by the following string of selections: Axial 2D -> Chemical Engineering Module -> Flow with Variable Density -> Weakly Compressible Momentum Transport -> k-ε Turbulence Model -> Transient Analysis. This process tree is shown in Figure 1 below. This selection was chosen after much thought and experimentation with other options including but not limited to the Weakly Compressible Navier-Stokes model and the k-ω Turbulence Model [4].

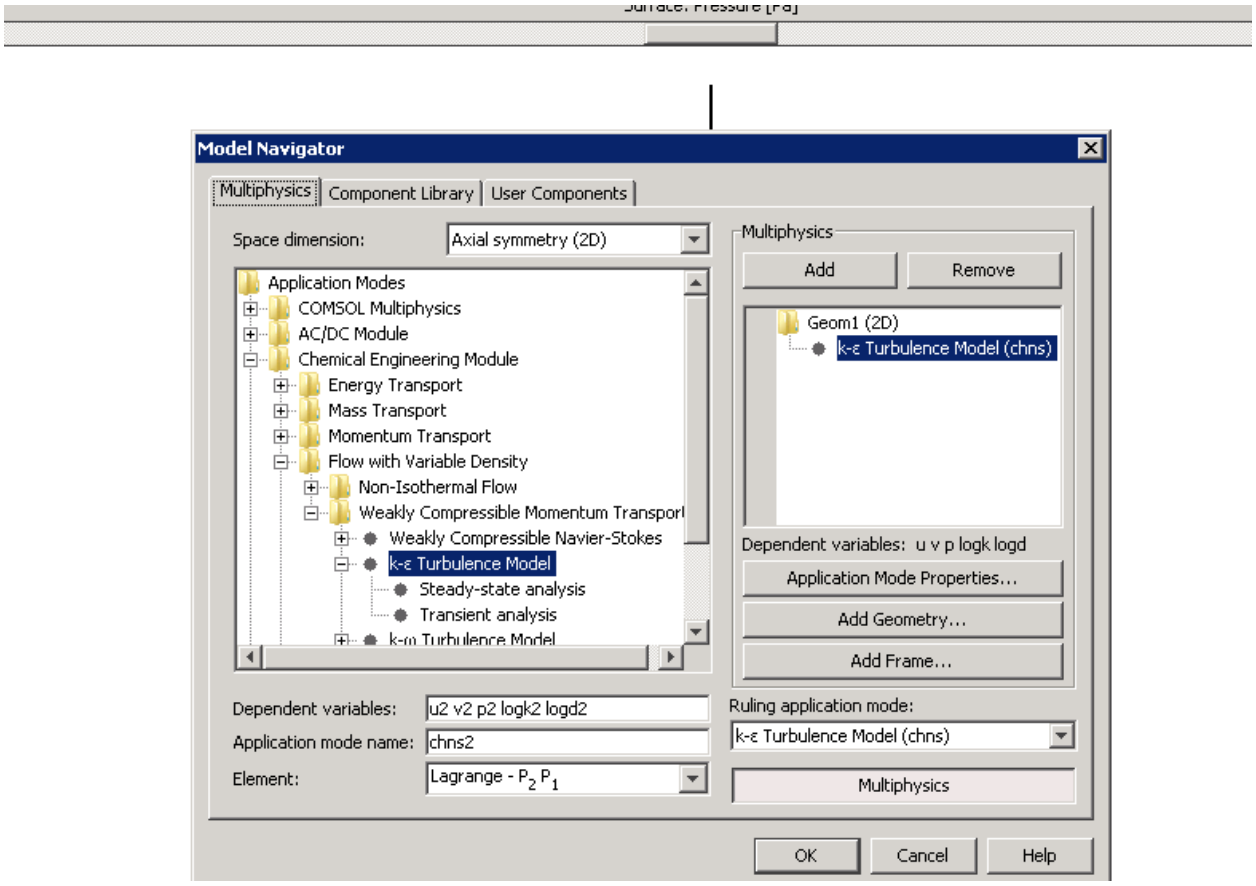

Figure 2: COMSOL Model Navigator Selection

Once the correct model was determined, the physical properties needed to be established. This took some experimenting with the program as there are several places and different ways to enter each value, and entering the value in the wrong place would give an error message that was undecipherable. The pressure gave lots of problems as far as what units it should be in, to what magnitude it should be set, and where it needed to be input.

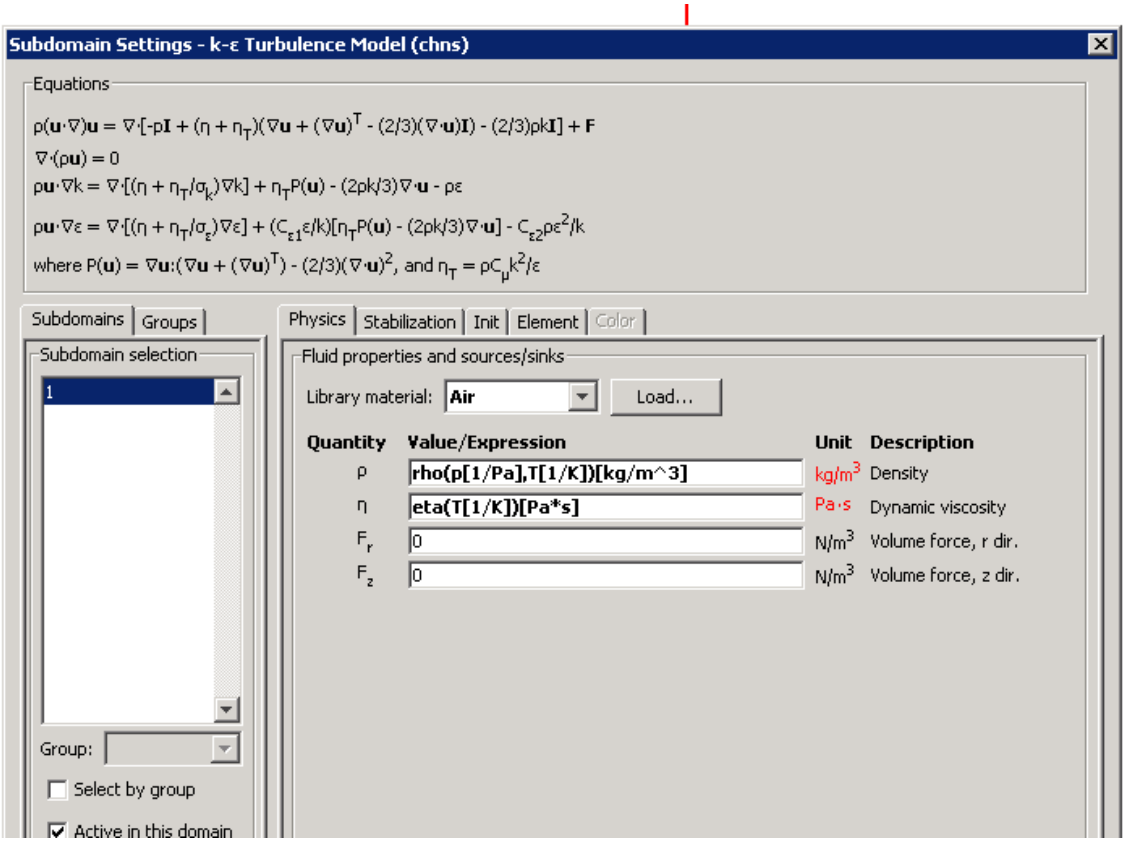

Figure 3: Setting the physics to be those of air

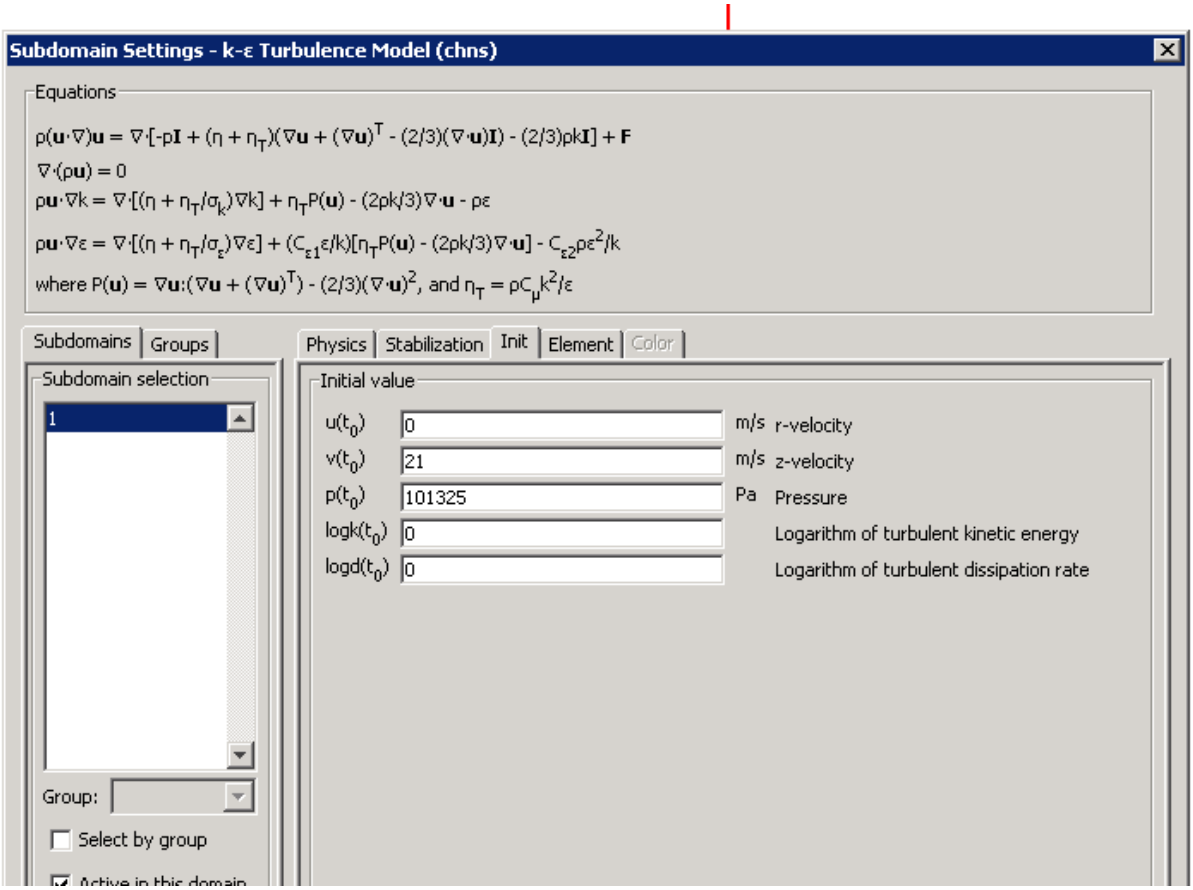

Figure 4: Setting the initial conditions to the system

The pressure was input as a boundary condition at the outlet, while the inlet condition was the velocity of the fluid flowing through the pipe. The central wall was set to be axially symmetric so as to provide a 3-D simulation of the pipe while showing a 2-D rectangle.

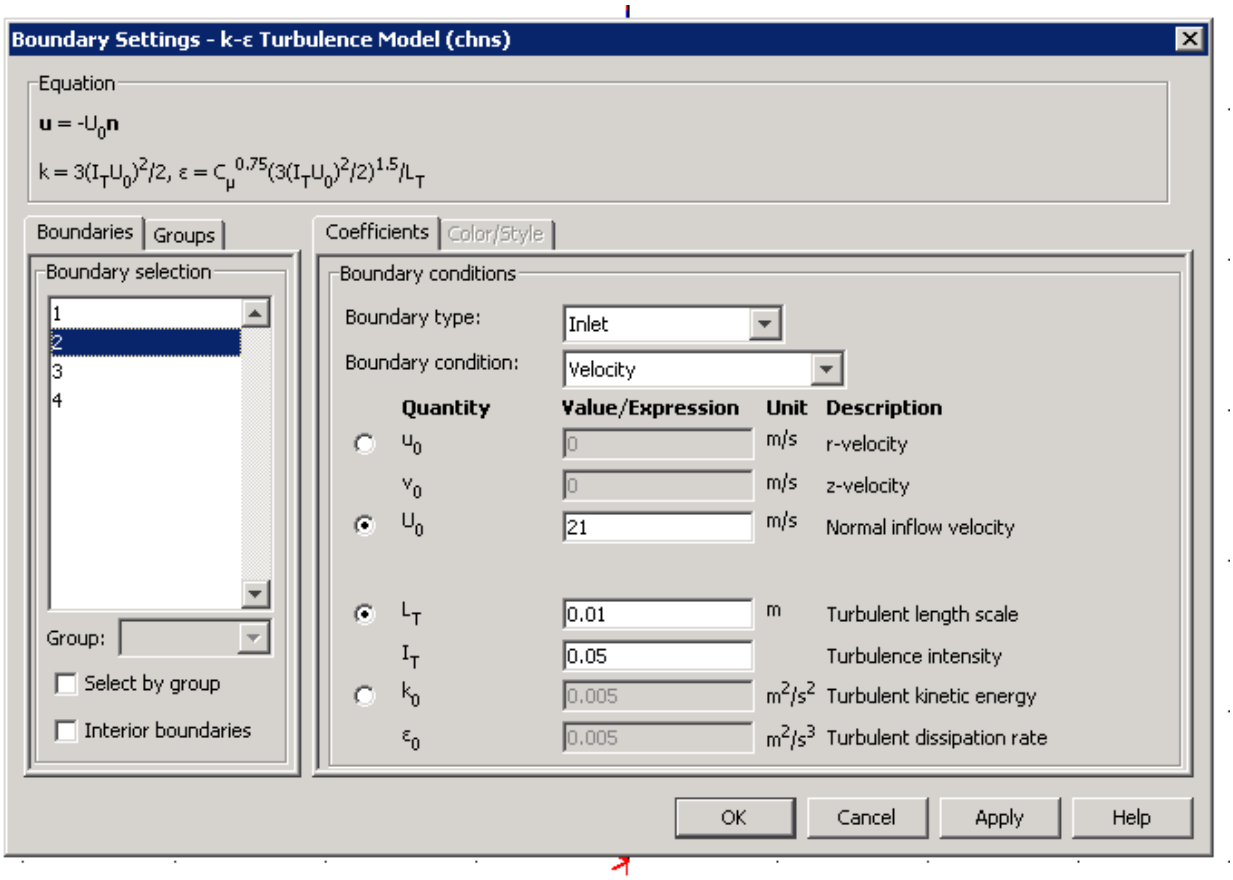

Figure 5: Setting the inlet boundary condition to velocity

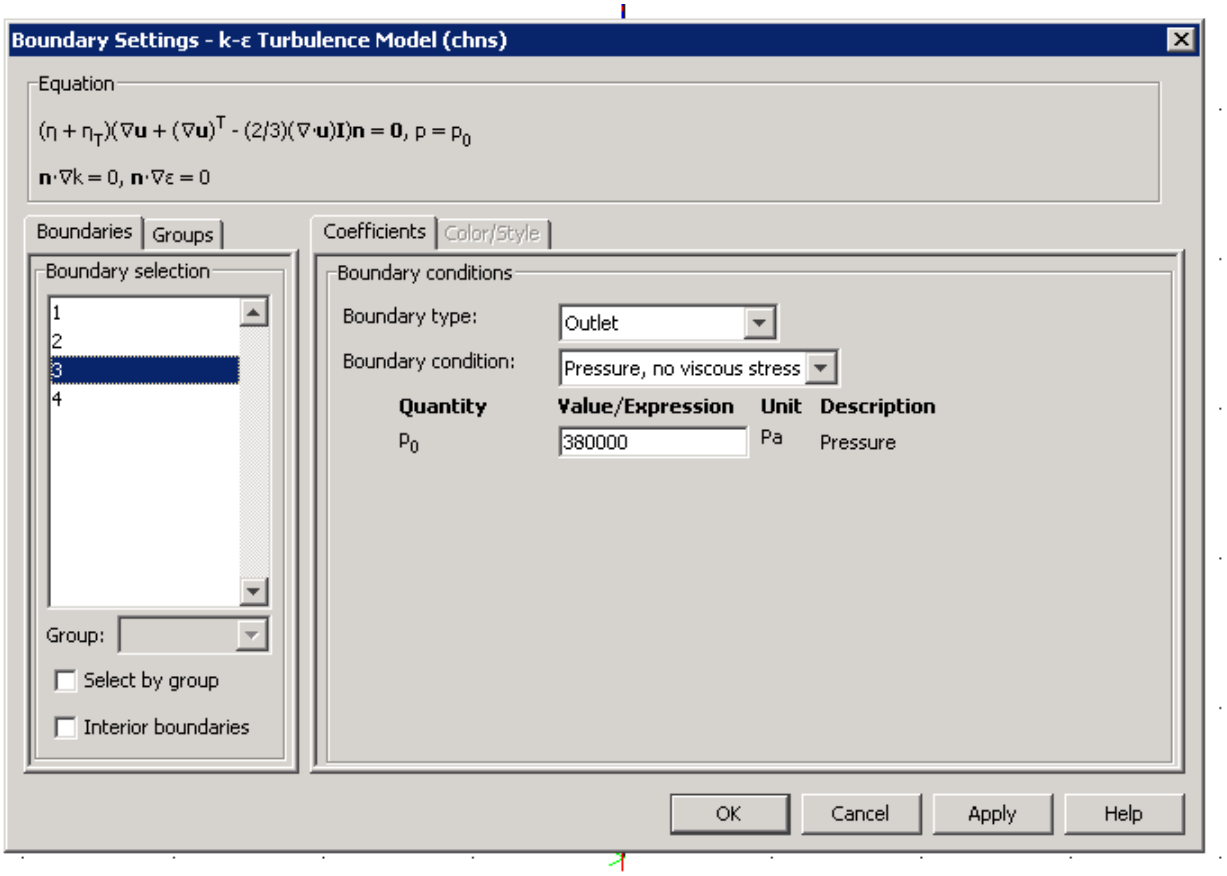

Figure 6: Setting the outlet boundary setting to be pressure

Once all the inputs were made correctly, the mesh of the object was defined and then refined in order to more accurately predict how the fluid would act in the pipe. The mesh was refined most specifically at the wall since the closer you get to the wall the more unpredictable the fluid becomes. The inlet mesh was also refined greatly in order to more accurately predict the way the pipe would act in real life.

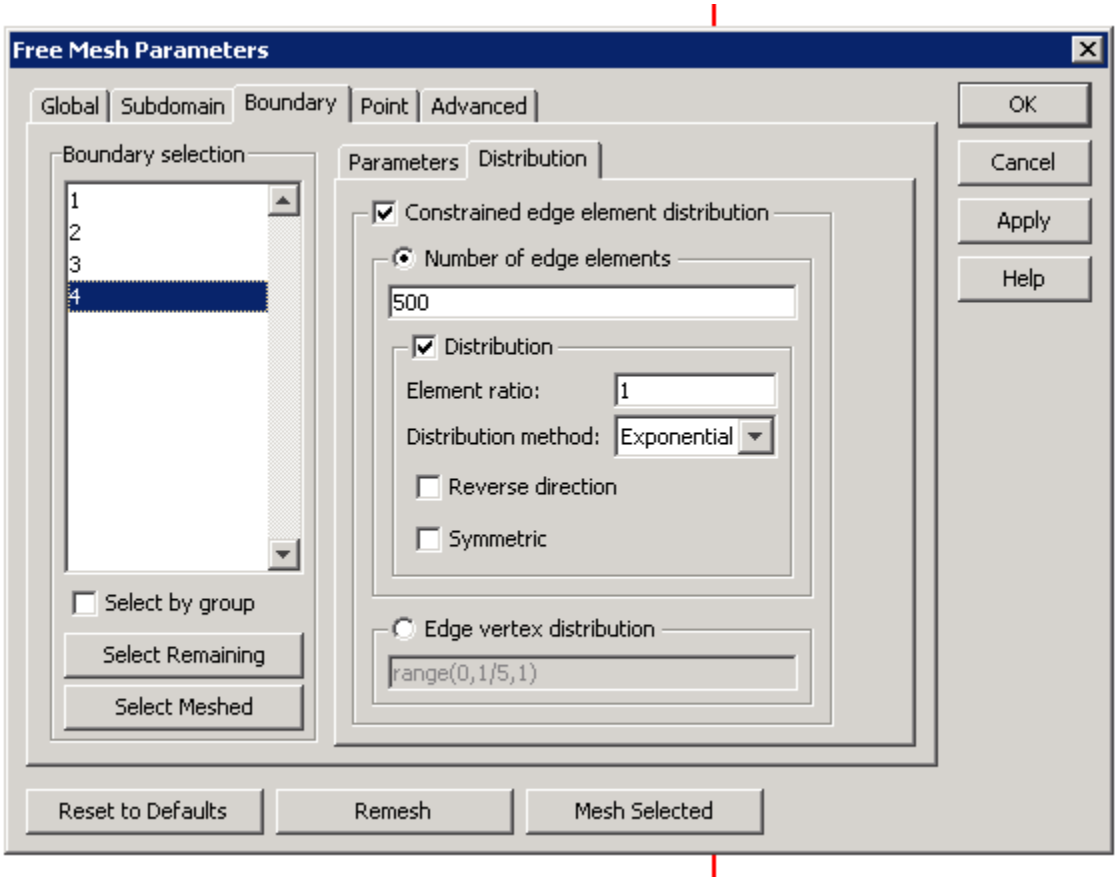

Figure 7: Refining the mesh at the wall

With the different values put into the system, the model can be run for different experiments. The results were examined using the post-processing techniques included with the program, specifically a boundary integration of pressure across several of the boundaries as well as a velocity profile. These are shown below.

Figure 8: Color variance shown in the model's display of pressure drop across the model

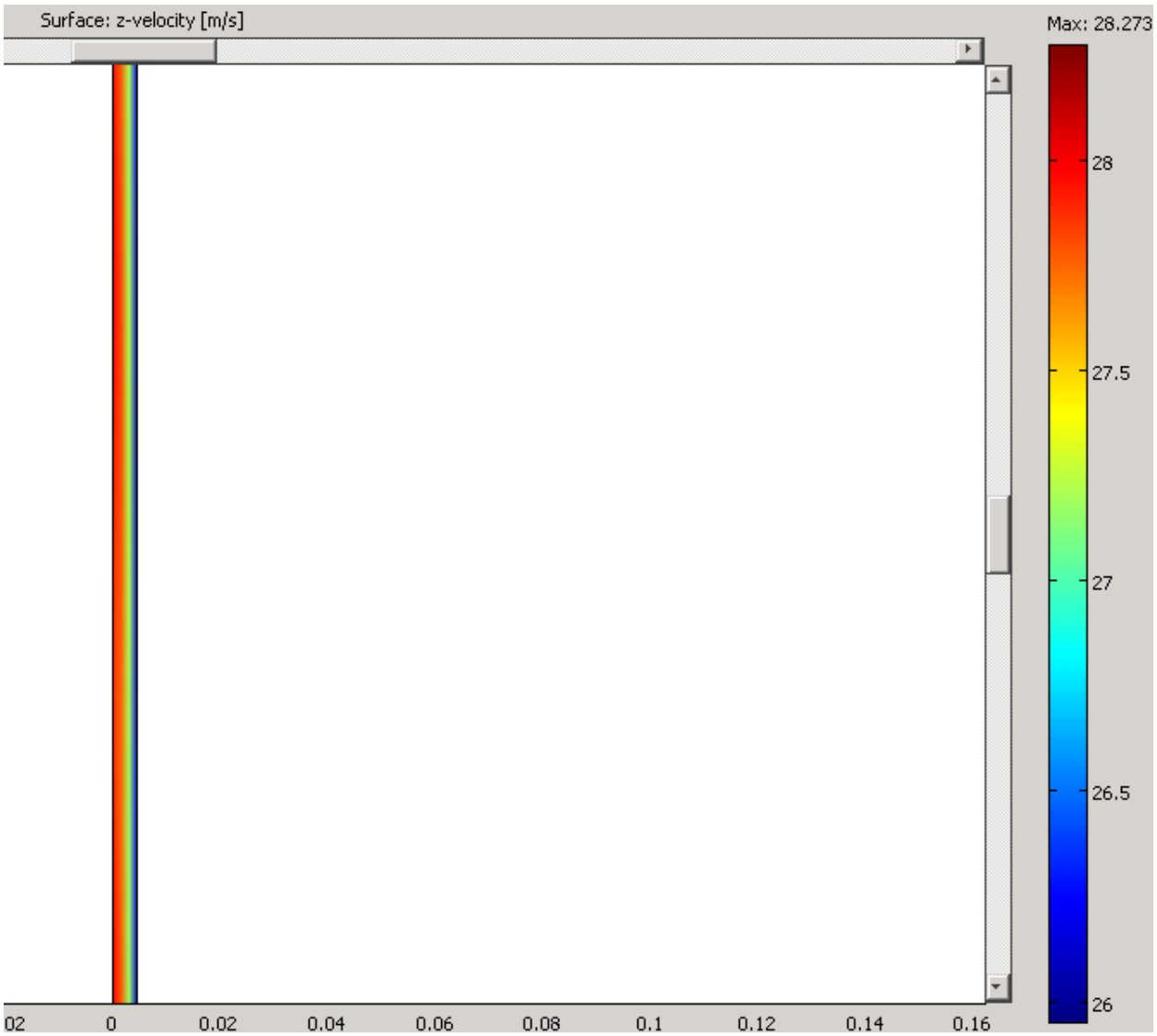

Figure 9: Color variance shown in the model's display of velocity across the model

The figure above shows that as the flow moves from the center to the outer edges of the pipe, the velocity drops several meters per second. This is due to the roughness at the pipe wall.

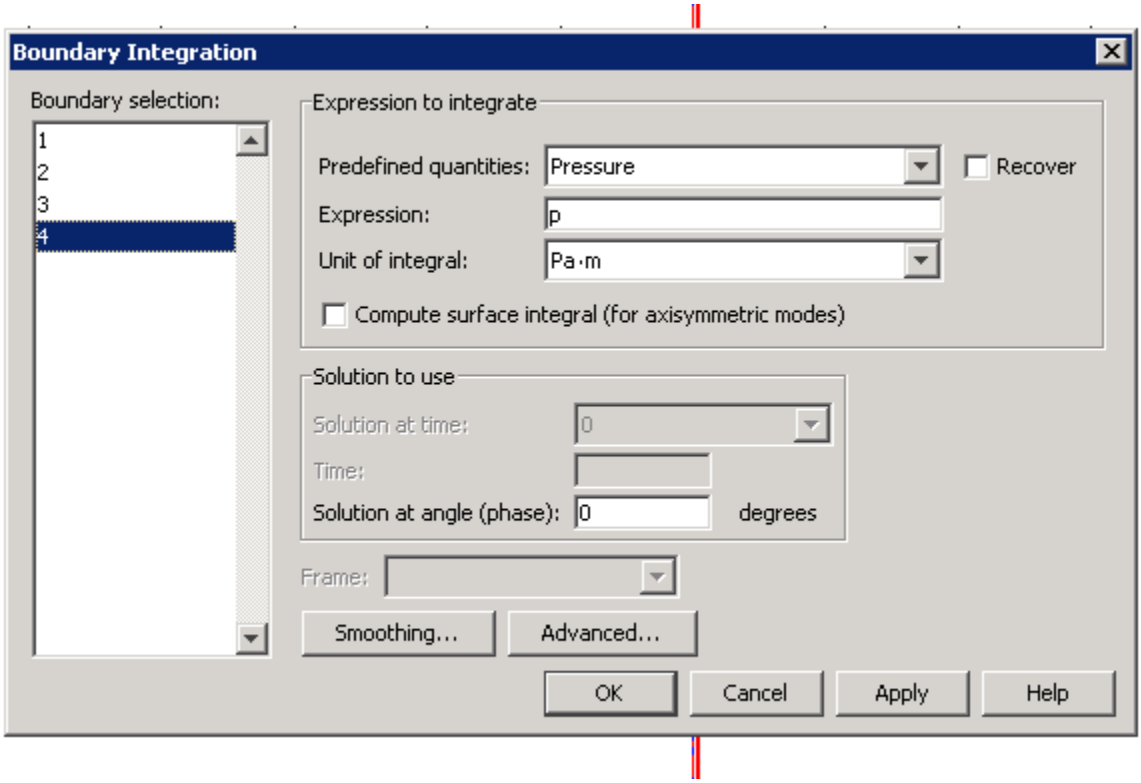

Figure 10: Boundary Integration feature of the Post-Processing function

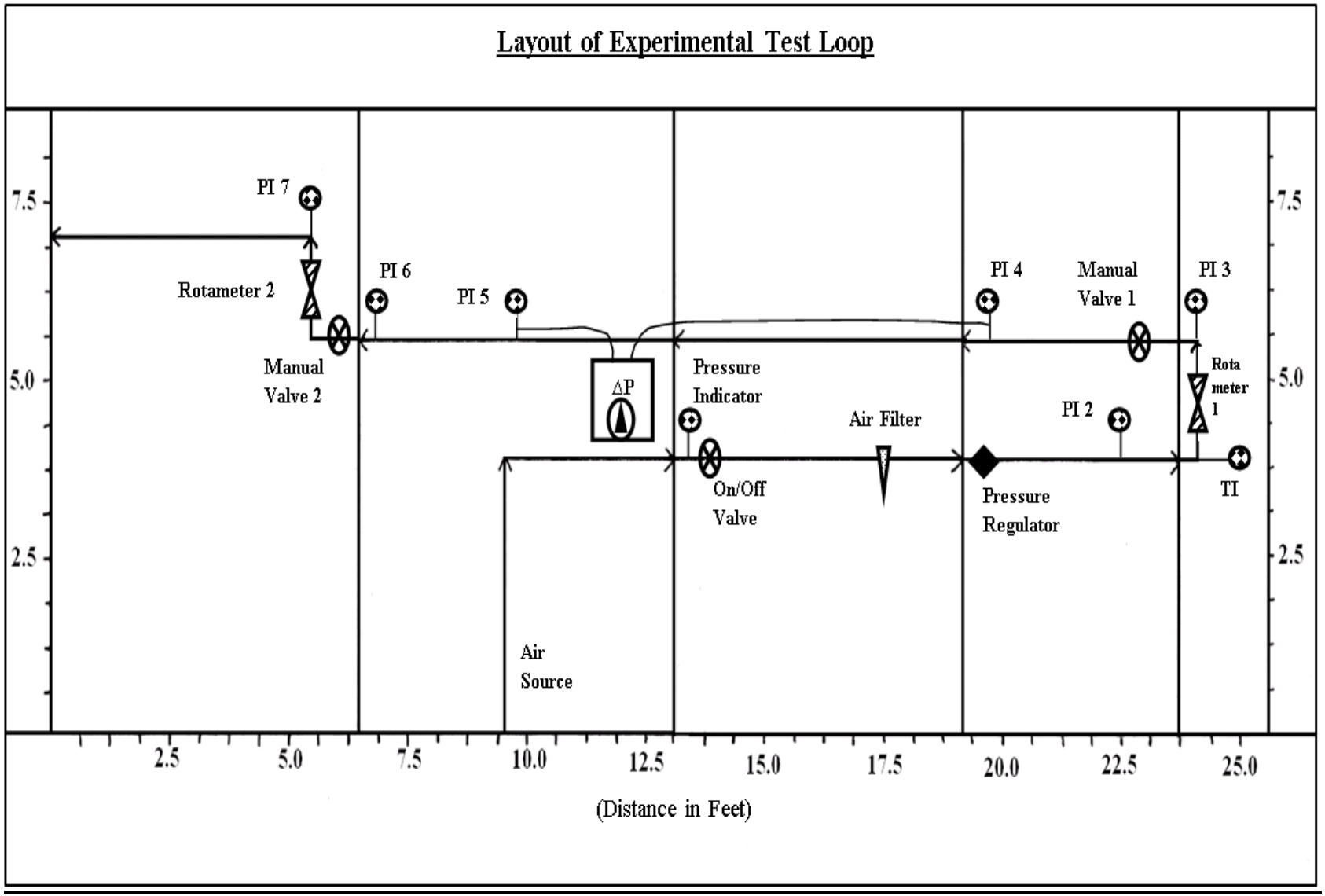

Figure 11: Layout of Experimental Loop

APPARATUS DESIGN AND CONSTRUCTION

The experimental apparatus was designed and constructed using the *Chemical Engineering Education* journal article as a guide. After assessing the ranges of data found in the article, the appropriate parts for our experiment were researched and selected accordingly. The individual pipe lengths were threaded in a machine shop and then assembled in the Unit Operations Lab with their corresponding gauges, meters, and valves. A complete parts list can be seen below. The final layout of the system can be seen above in the "Layout of Experimental Test Loop" schematic. The function of each part is detailed in the process description seen below.

PARTS LIST [7]

- **Pressure Indicator 1 and 2** = Dwyer, Series SGI, Stainless Steel, Safety Pressure Gauge, 0 – 150 psi, Model # SGI – F0624N, $75.00 each.
- **On/Off Valve** = Grainger, 1/4 inch Ball Valve, Seal Weld, 6000 psi, Stainless Steel, Sharpe Valves Brand, Model # 50F76, $119.20.
- **Air Filter** = Dwyer, Series AFR, Air Filter Regulator, 0 – 120 psi, 1/4 inch connection, Model # AFR4, $49.50.
- **Pressure Regulator** = Omega, 1/4 inch, Precision Pressure Regulator, 2 – 60 psig, Dial Gauge, Hand Wheel Adjustment, Model # PRG501 – 60, $450.00.
- **Temperature Indicator** = Dwyer, Bimetal Thermometer, 2 inch dial, 1/4 inch NPT, 0 - 250F, Model # BTB22551, $35.00.
- **Rotameter 1** = Dwyer, Series UV, Ultra View Polysulfane Flowmeter, 1 – 13 SCFM air, Model # UV – A112, $173.00.
- **Rotameter 2** = Dwyer, Series UV, Ultra View Polysulfane Flowmeter, 2.5 - 28 SCFM air, Model # UV – B112, $173.00.
- **Pressure Indicator 3, 4, 5, 6 and 7** = Dwyer, Series SGI, Stainless Steel, Safety Pressure Gauge, 0 – 100 psi, Model # SGI – F0524N, $75.00 each.
- **Manuel Flow Valve 1 and 2** = Dwyer, Series HGV, Stainless Steel, Hand Operated Globe Valve, 1/4 inch, C_V = 0.6, Model # HGV00, $29.50 each.
- **Pipe** = Grainger, 1/4 inch, Stainless Steel, Schedule 40, 10ft lengths, Sharon Piping Brand, Model # 70BWP406L, $85.00 each.
- **Differential Pressure Gauge** = Dwyer, Series 4000, Capsuhelic Differential Pressure Gauge, 4 inch dial, 1/4 inch connection, 0 – 50 in water, Model # 4050, $366.00.

PROCESS DESCRIPTION

First, the “Air Source” is turned on, releasing pressurized air into the system at 85 psig. The air then flows through the schedule 40, 1/4 inch pipe for 4 feet. The pressure of the air at this point is measured and indicated by "Pressure Indicator 1". The air is then allowed to continue through the system by the "On/Off Valve" when it is in the opened position. Next the air is filtered through the "Air Filter" to remove moisture and unwanted particles. The pressure of the air is then controlled and set to a desired pressure using the "Pressure Regulator". Next the pressure and temperature of the air are measured by "Pressure Indicator 2" and "Temperature Indicator" respectively. The air then flows vertically into "Rotameter 1" where the volumetric flow rate of the air is measured and indicated in SCFM. The pressure of the air is then measured by "Pressure Indicator 3". Next the flow can be adjusted manually by "Manuel Flow Valve 1" using a hand turned dial. The air then continues to flow for 3 ft. before it reaches the 10 ft. length of pipe over which the pressure drop will be measured. At the start and end of this 10 ft. pipe the pressure is measured by "Pressure Indicator 4" and "Pressure Indicator 5" respectively. Plastic tubes tap these 2 pressure gauges and connect them to the "Differential Pressure Gauge" where the pressure drop across the 10 ft. length of pipe is calculated and displayed. The "Differential Pressure Gauge" is mounted to a panel located below the pipe and in between PI4 and PI5. The air then flows for another 3 ft. where the pressure is measured again by "Pressure Indicator 6". Next the flow of the air can be manually adjusted again by "Manuel Flow Valve 2" before flowing vertically into "Rotameter 2". This rotameter measures the volumetric flow rate of the air in the same way as "Rotameter 1". Finally the pressure of the air is measured by "Pressure Indicator 7" and allowed to flow out of the system.

Experimentation and Calculations

To begin the experimental runs of the apparatus, the team determined what they would find and how. It was determined that the mass flow rate, Reynolds number and Darcy friction factor should be solved for using calculation. The volumetric flow rate, density and pressure drop would also need to be found but depended on experimental results. After the initial experiments, several calculations were also needed to make the data compatible with COMSOL. The procedures used follow below.

Mass and Volumetric Flow Rate

For the first set of experiments, the team chose several different mass flow rates to keep consistent in order to see the trend that occurs as the pressure is increased at a constant flow rate. Due to this, the volumetric flow rate needed to be calculated for each run before anything else could be done. The volumetric flow rate was calculated using the desired mass flow rate, the pressure of the system and the calibration density of air. The equations used are as follows[1]:

$$F_{actual}^{mass} = F_{cal}^{mass}\sqrt{\frac{P_{actual}}{P_{cal}}} \qquad (6)$$

$$F_{cal}^{mass} = F_{cal}^{vol} * \rho_{cal} \qquad (7)$$

Where F is the flow rate and the super scripts mass and vol stand for either mass flow rate or volumetric flow rate. The volumetric flow rate term is calculated, not calibration. The ρ_{cal} term is the density of air used to calibrate the rotameters. This term is calculated using standard temperature and pressure and remains constant throughout the experiments.

For this experiment's purposes, the actual mass flow rate was set prior. This value was used with the difference in pressures to find the calibration mass flow rate. The calibration mass flow rate was then used along with the calibration density of air to calculate the volumetric flow rate.

The volumetric flow rate calculated was then used as a starting point for each experiment. The rotameter was set to these values and the pressure drop between the rotameter and the ten foot length of pipe was recorded. This provided approximately the actual pressure that the system would be operating at. Using the difference in pressures then, the volumetric flow rate for the rotameter was set so that the corrected volumetric flow rate would be the one specified earlier to have a certain mass flow rate. The equation used is shown below[1]:

$$Q_2 = Q_1\sqrt{\frac{P_1}{P_2}} \qquad (8)$$

Where Q_2 is the volumetric flow rate at the ten foot pipe, Q_1 is the volumetric flow rate at the rotameter, and each P is the corresponding pressure to those locations. This equation differs from equation six in that it is volumetric flow rate and it also solves the equation between two experimental pressures while equation six finds a pressure based on the values used to calibrate the rotameter.

Pressure Drop

The pressure drop across the ten foot length of pipe in the experiment was determined using the differential pressure gauge installed on the system. This value was then multiplied by 27.7 in order to get the pressure drop in pounds per square inch. This was necessary to compare this experiment's results with those in the chemical engineering journal. These values were also used in creating a graphical representation of the data.

Density

The density of air in each individual experiment was calculated using a variation of the ideal gas law that includes density. For this calculation, the pressure directly after the rotameter was taken to ensure the density was calculated using the pressure closest to the ten foot length of pipe [1].

$$\rho = \frac{P*MW}{RT} \qquad (9)$$

Entry Length

The entry length for the pipe needed to be calculated for each experiment to determine what length of pipe would lead up to the ten foot length. This entry length would provide that the flow of air in the pipe would be fully developed flow and therefore turbulent. Having fully developed flow was a necessity to be sure the experimental results would be consistent from run to run. The equation used is shown below [2].

$$L = 4.4 * Re^{\frac{1}{6}} * D \qquad (10)$$

Where L is the entry length, Re is the Reynolds number and D is the diameter of the pipe.

Calculating values for COMSOL from Experimental Results

In order to make comparisons between COMSOL and the experiments performed in lab, the correct values for pressure and velocity needed to be calculated prior to entering them into COMSOL.

Velocity

COMSOL has a default to require a velocity in meters per second. In order to solve for this a calculation was done involving several conversion factors, the cross-sectional area of the pipe and the corrected volumetric flow rate. The equation used is shown below [2]:

$$V = \frac{F_{Actual}^{Vol}}{A} * \frac{1}{60*3.048} \qquad (11)$$

Where V is velocity, A is cross sectional area, F is the corrected volumetric flow rate ft^3/min, 1/60 is a conversion from minutes to seconds and 1/3.048 is a conversion from feet to meters.

Pressure

The default units for pressure in COMSOL are pascals, and the pressure is an absolute pressure. As such the pressure given by the apparatus must be converted to be the same. The equation used is shown below [4]:

$$P_{Pa} = P_{psi} * 6894 + 101325 \qquad (12)$$

Where P_{pa} is the absolute pressure in pascals, P_{psi} is the gauge pressure in psi, 6894 is the number of pascals in a psi and 101325 is the number of pascals at atmospheric pressure.

Results and Discussion

Experimental Results

Once completing the experiment, the group plotted the pressure of the flow versus the pressure drop at different flow rates. Because the goal of the experiment was to match up these new results with the published document, the data from the other document is also plotted in the figure below.

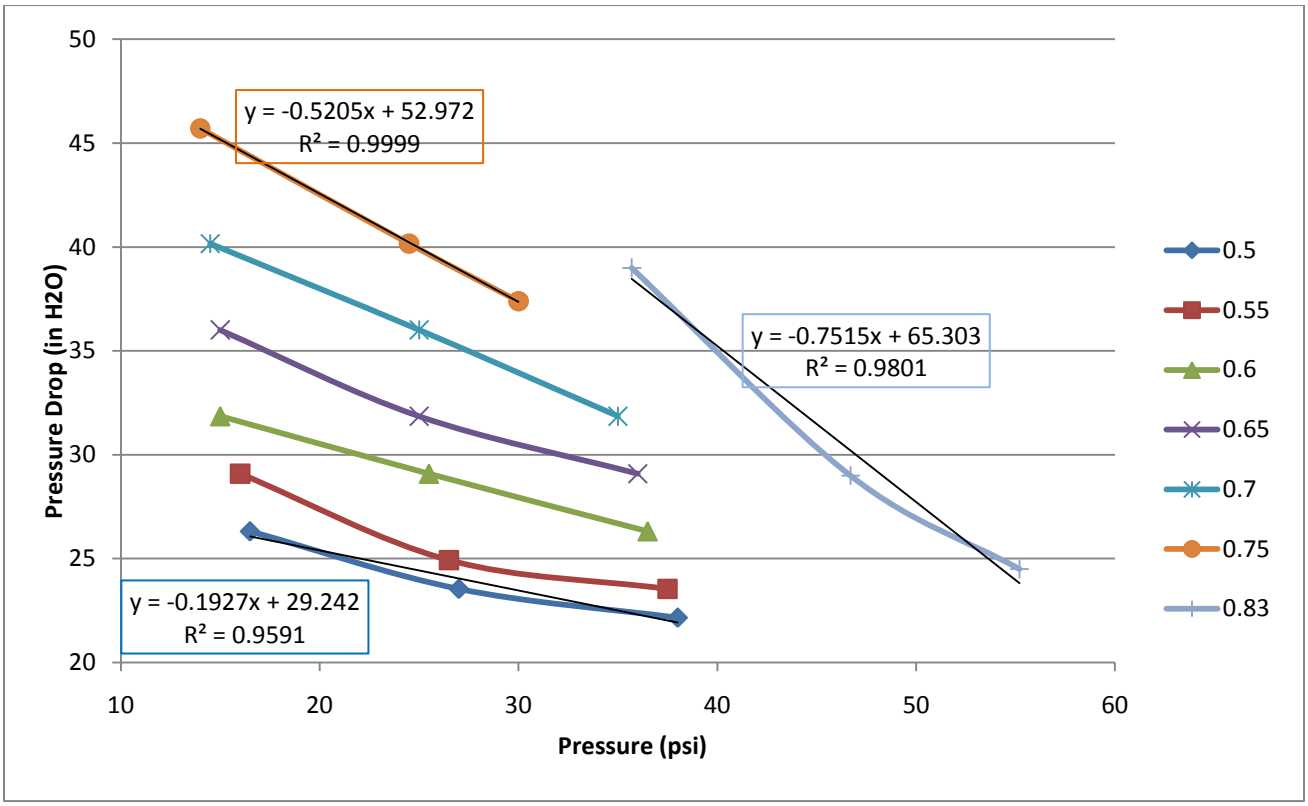

Figure 12: Pressure vs. Pressure Drop at Varying Mass Flowrates (Experimental)

As can be seen in the plot above, there is an obvious trend where the pressure drop decreases with increasing pressure. As the mass flow rate rises, the amount of pressure drop in the flow decreases at an increasing rate as the pressure increases. This is because with an increasing mass flow rate, the velocity increases. With a higher pressure, the density increases and the velocity decreases. Because velocity has more of an effect on the pressure drop than the density, the pressure drop at higher mass flow rates declines at a noticeably higher rate.

Due to limitations with the apparatus that was constructed, it was not possible to attain data at the mass flow rate used in the document that was being emulated. Mass flow rates at the same pressures were also very difficult to obtain due to limitations. In trying to attain a mass flow rate at a very high pressure, the volumetric flow rate would rise to the point that there was no

back pressure and the pressure within the system would drop. In trying to get a mass flow rate high enough to compare to the paper, the team decided to use three pressures that would be applicable at many different mass flow rates and try to get as close to the paper's data as possible. Thus the higher pressures that the paper used were not applicable to this apparatus. At the pressures in the paper, the low mass flow rates would show essentially the same pressure drops to other mass flow rates given the same trends.

In the graph above, the data for 0.83 lb_m/min is at pressures of roughly one atmosphere, or 14.7 pounds per square inch, higher than the team's data. However, one can see that if the data was recorded at the pressures the team used and still followed the same trend line, it would fit well with the data attained by the team. The flow rate is slightly higher than the highest flow rate that the team used, and the rate at which the pressure drop decreases is also slightly higher than that of 0.75 lb_m/min. If a new pressure regulator could be purchased, then it is very possible that the experiment could be repeated and fit the trend well.

COMSOL Results

Once the COMSOL model was fully set up, it was run several times for each experimental run in the lab. The velocity and the pressure that were calculated from experimental data for use within the model were input for each situation and the results produced several trends.

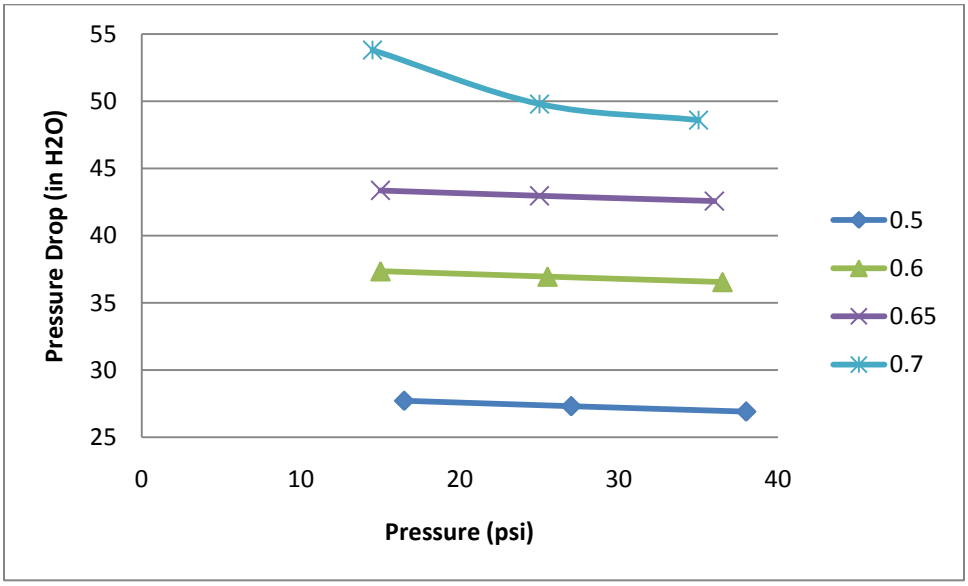

Figure 13: Pressure vs. Pressure Drop at Varying Mass Flowrates (COMSOL)

As can be seen in the above graph, the COMSOL data shows the same general trend as the experimental data when it comes to pressure vs. pressure drop. As the pressure of the system increases, the pressure drop across the pipe decreases. This is exhibited more closely in the graph below which shows only the runs at 0.65 and 0.7 lb/min.

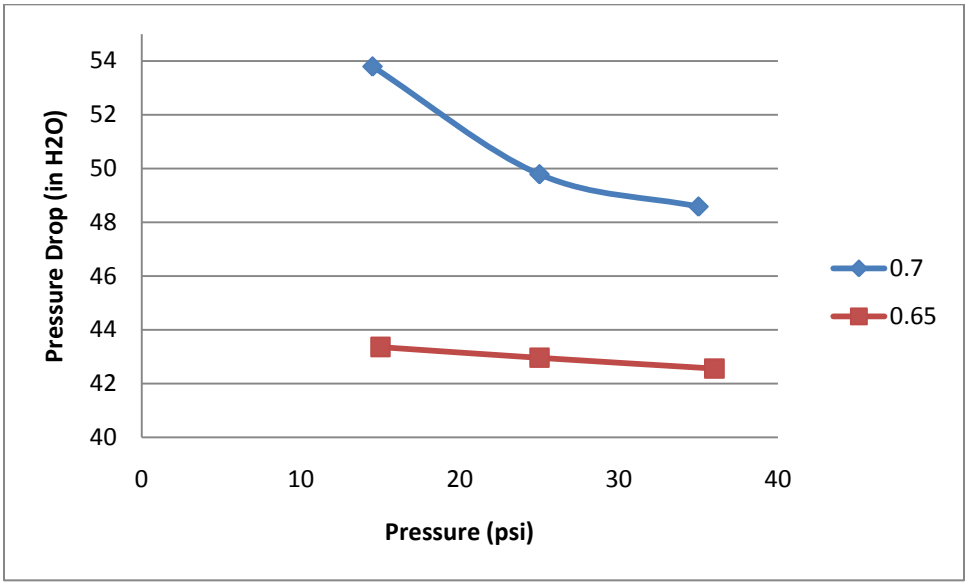

Figure 14: Pressure vs. Pressure Drop at 0.65 and 0.7 lb/min (COMSOL)

A second trend that should be noted is that as the velocity increased within a constant mass flow rate, the pressure drop also increased. An increase in velocity in the system coincides with a decrease in pressure, so this makes sense on both accounts.

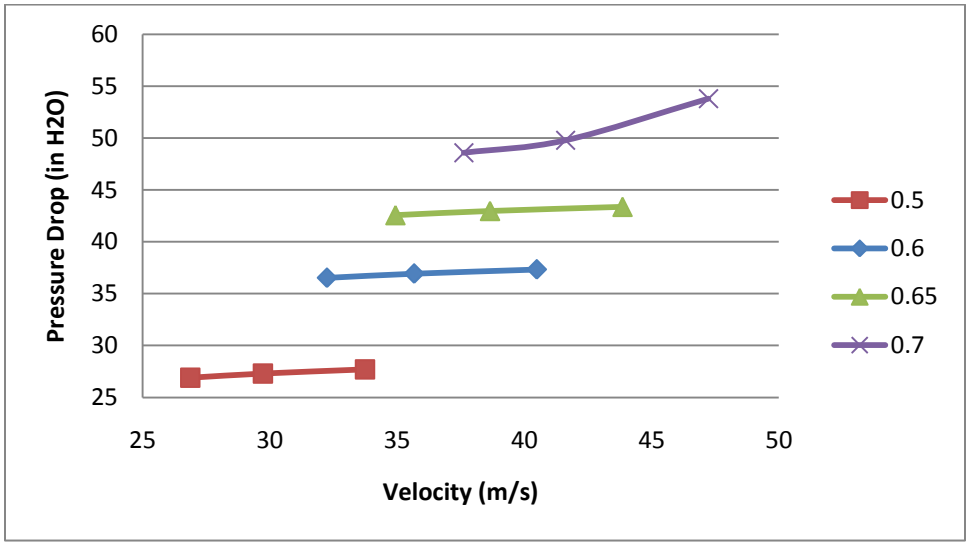

Figure 15: Pressure Drop vs. Velocity at Varying Flow Rates

As can be seen above and more closely below, there is a clear trend in the pressure drop getting larger as the velocity in the system increases.

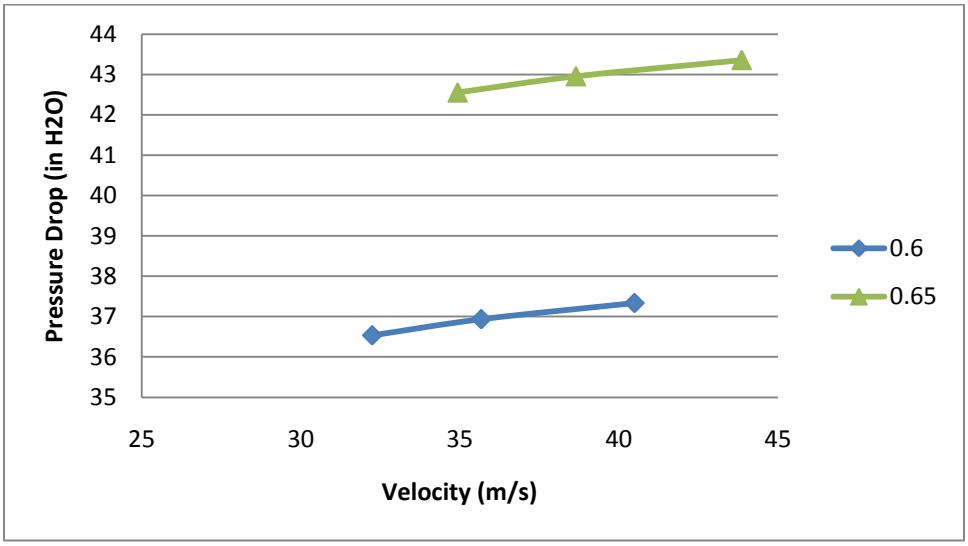

Figure 16: Pressure Drop vs. Velocity at 0.6 and 0.65 lb/min (COMSOL)

Differences between Mass Flow Rates

When looking at the data acquired from running the experiment, the group found that while keeping a constant mass flow rate and setting the pressure regulator to a certain pressure, there would be a certain pressure drop across the pipe. If the pressure regulator was set to a lower pressure while keeping the mass flow rate the same, the pressure drop would rise. If the reverse was to be done, raising the pressure and keeping the mass flow rate the same, the pressure drop would decrease from its previous value.

If the set pressure is lowered, then the compressible gas would have a higher velocity through the pipe. The higher the velocity becomes, the more the pressure drop increases due to its part in the pressure drop formula [2]:

$$\Delta P = \frac{v^2 \times f \times L \times \rho}{2D} \qquad (13)$$

As is shown above, the velocity is squared in the equation for pressure drop. This counteracts the friction factor and density decreasing as the pressure drops, and causes the overall pressure drop across the pipe to increase.

If the mass flow rate was increased while keeping the same pressure, the pressure drop would increase as well. Following that trend, if the mass flow rate was decreased the pressure drop would decrease as well. This is because as the mass flow rate is increased the velocity is also

increased, and as the explanation above tells, the pressure drop will rise as the velocity increases.

Rotameter Inaccuracy

When calculating the experimental results, the team came across a problem. The two rotameters were reading different volumetric flow rates. After use of the below equation, it became clear that the two rotameters disagreed greatly on what the flow rate was. The team based all its calculations on the reading of the first rotameter to avoid any undue differences in the numbers [1].

$$Q_2 = Q_1\sqrt{\frac{P_1}{P_2}} \qquad (14)$$

The inaccuracy of the second rotameter is shown on the graph below. The rotameter consistently read higher than what it should have to represent what the flow rate was through the pipe.

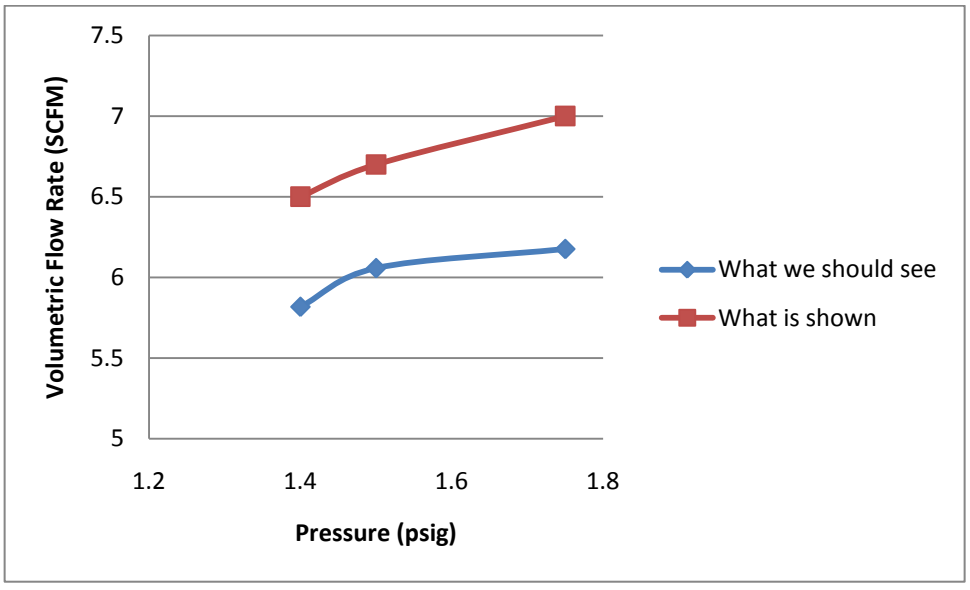

Figure 17: 2nd Rotameter Inaccuracy at 0.5 lb/min

COMSOL Results vs. Experimental Results

The COMSOL and experimental results showed many of the same trends. The main difference is that the experimental results show a much more dramatic change in pressure drop when the pressure is changed. This is shown in the following graphs.

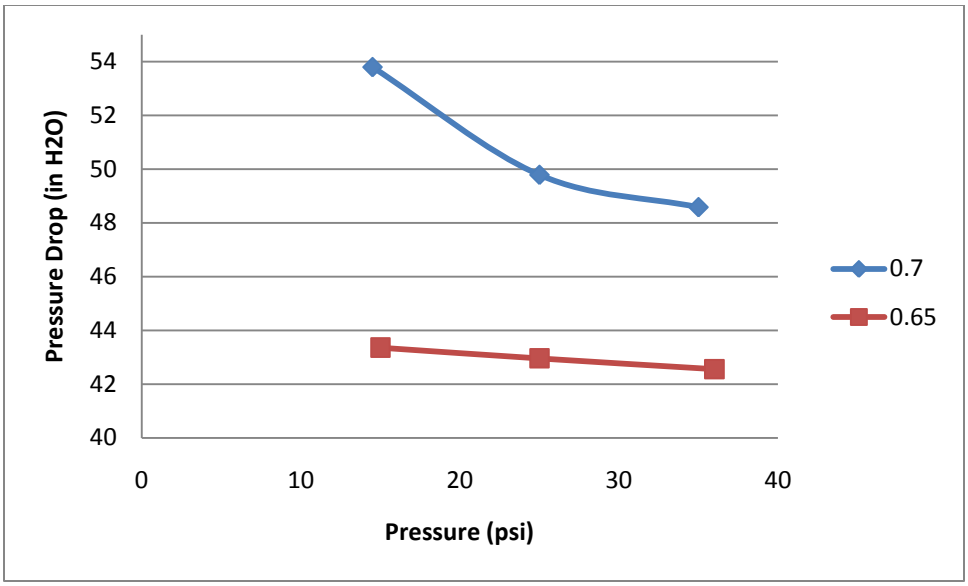

Figure 18: Pressure vs. Pressure Drop at 0.65 and 0.7 lb/min (COMSOL)

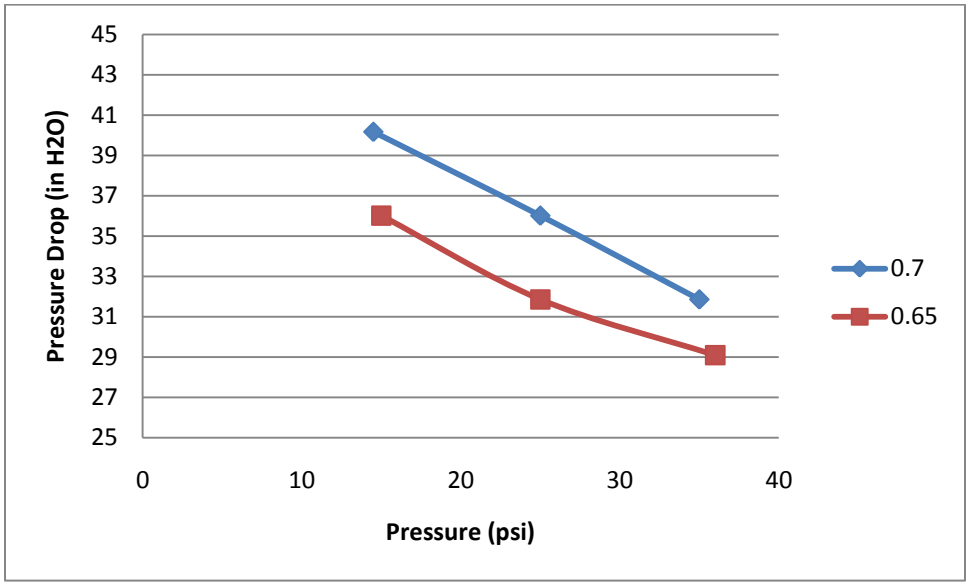

Figure 19: Pressure vs. Pressure Drop at 0.65 and 0.7 lb/min (Experimental)

As the above graphs show, the pressure drop is higher in the COMSOL model. The data also shows that as the pressure is increased, the pressure drop across the pipe rises. While this trend is shown by both sets of data, the COMSOL data at a mass flow of 0.65 lb/min drops 1 inch of water and the experimental data show a drop of 8 inches of water for the same pressures and flow rate. These two sets of data are shown below in the same graph for comparison.

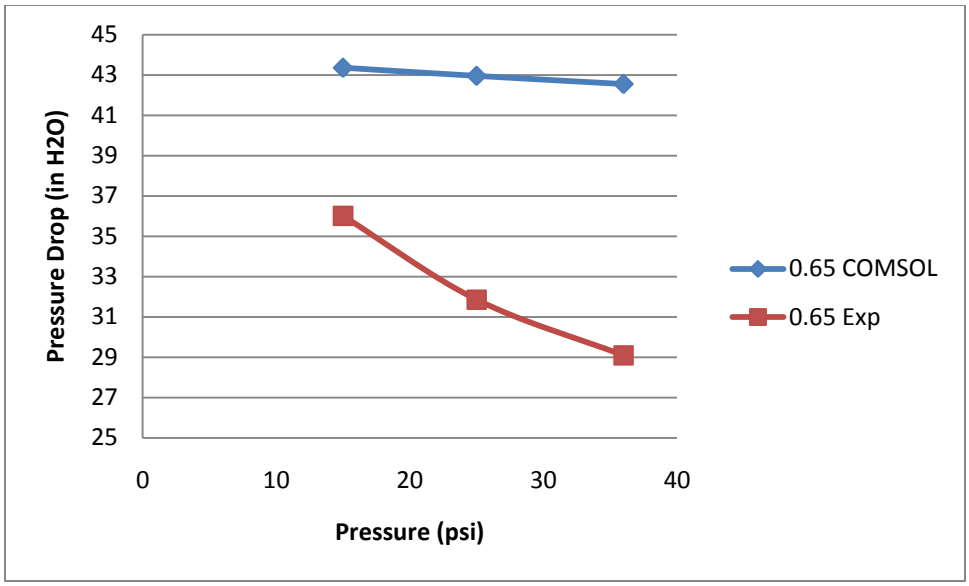

Figure 20: Pressure vs. Pressure Drop at 0.65 lb/min COMSOL vs. Experimental

The same comparison can be made using pressure drop versus velocity in the COMSOL and experimental data. As the velocity increases, so too does the pressure drop. While both sets of data show this trend, the experimental data once again has a greater difference between each datum. These data are shown below. The third graph shows a comparison between the experimental and COMSOL data at the same mass flow rate.

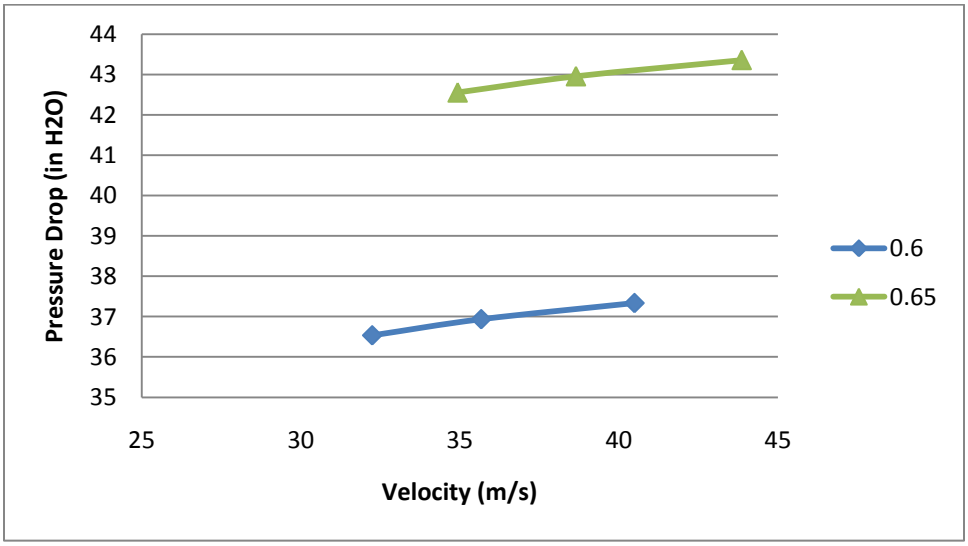

Figure 21: Pressure Drop vs. Velocity at .6 and .65 lb/min (COMSOL)

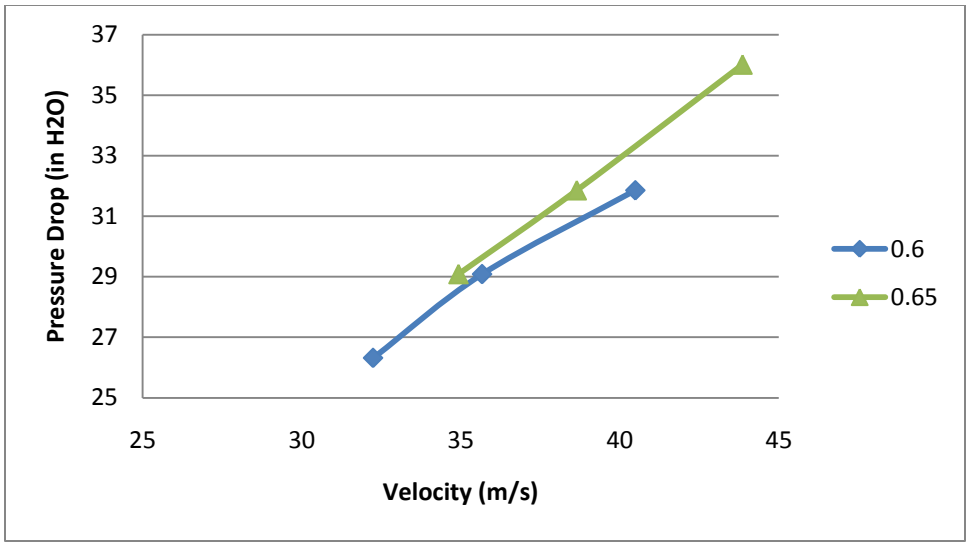

Figure 22: Pressure Drop vs. Velocity at 0.6 and 0.65 lb/min (Experimental)

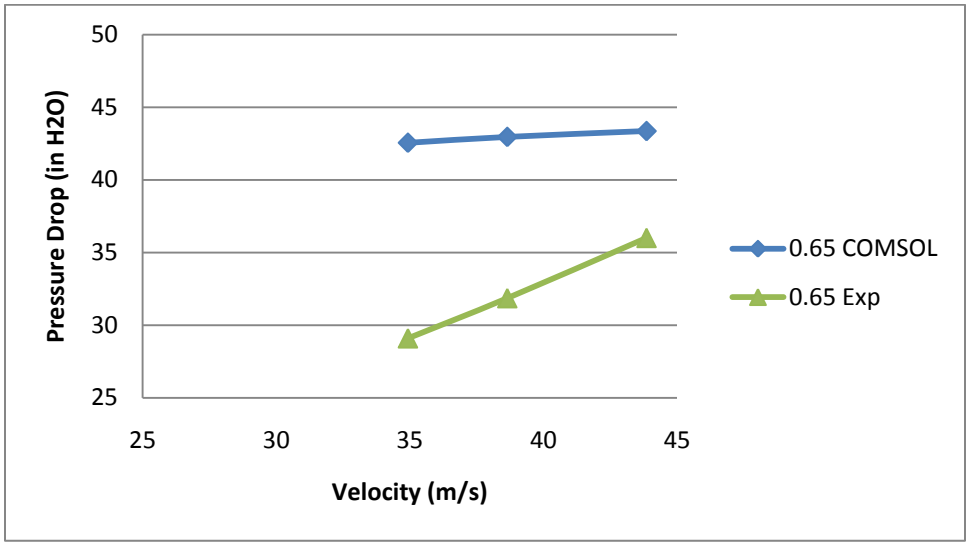

Figure 23: Pressure Drop vs. Velocity at 0.65 lb/min COMSOL vs. Experimental

Reynolds Number

In order to calculate the Darcy friction factor and pressure drop of the flow, the Reynolds number must first be determined. Using the equation for finding the Reynolds number found in the background of this document, the results for each flow can be seen in the table below.

Table 1: Reynolds Numbers at varying Densities and Velocities

Flow Rate (lb_m/min)	Pressure (psi)	Density (lb_m/ft^3)	Velocity (ft/sec)	Diameter (ft)	Dynamic Viscosity (lb_f*s/ft^2)	Reynolds Number
0.5	38	1.936E-01	59.6	3.03E-02	3.82E-07	28464
0.5	27	1.376E-01	83.8	3.03E-02	3.82E-07	28464
0.5	16.5	8.408E-02	137.2	3.03E-02	3.82E-07	28464
0.55	37.5	1.911E-01	66.4	3.03E-02	3.82E-07	31310
0.55	26.5	1.350E-01	93.9	3.03E-02	3.82E-07	31310
0.55	16	8.153E-02	155.6	3.03E-02	3.82E-07	31310
0.6	36.5	1.860E-01	74.4	3.03E-02	3.82E-07	34157
0.6	25.5	1.299E-01	106.5	3.03E-02	3.82E-07	34157
0.6	15	7.643E-02	181.0	3.03E-02	3.82E-07	34157
0.65	36	1.834E-01	81.7	3.03E-02	3.82E-07	37003
0.65	25	1.274E-01	117.7	3.03E-02	3.82E-07	37003
0.65	15	7.643E-02	196.1	3.03E-02	3.82E-07	37003
0.7	35	1.783E-01	90.5	3.03E-02	3.82E-07	39849
0.7	25	1.274E-01	126.7	3.03E-02	3.82E-07	39849
0.7	14.5	7.389E-02	218.5	3.03E-02	3.82E-07	39849

At each flow rate in the range of 0.5 lb_m/min to 0.7 lb_m/min, it is evident that the flow is turbulent. As the flow rate increases, the Reynolds number also increases. Using these Reynolds numbers, the Darcy friction factor can now be found.

Darcy Friction Factor

The Darcy friction factor is an important quantity used in the calculation for pressure drop. It can be calculated using several methods:

1. Using a Moody diagram
2. The Colebrook Equation
3. The Haaland Equation
4. The Swamee-Jain Equation

Depending on the importance of time and accuracy, the desire to use each method could change.

1. Moody diagram
   Using a Moody diagram factor is by far the quickest and easiest method in determining the Darcy friction factor, though it is the least accurate. Using the Reynolds number as well as the relative roughness of the pipe, the friction factor can be found by following

the curves on the chart. Because the pipe is made of stainless steel, the roughness was determined to be 4.92E-5 feet, giving a relative roughness of 0.0015. Using this method, the friction factors all vary from around 0.026 to 0.027, but since the points are so close together it is impossible to have more accurate results from just looking at the chart.

2. The Colebrook Equation

The Colebrook equation solves for the Darcy friction factor implicitly rather than directly. Using the equation below, the group attempted to find the best value for *f* using Excel's Goalseek function [2].

$$\frac{1}{\sqrt{f}} = -2\log_{10}\left(\frac{\varepsilon/D_h}{3.7} + \frac{2.51}{Re\sqrt{f}}\right) \qquad (3)$$

First, the team set up a table with columns for the flow rate, friction factor, left side of the equation, right side of the equation, and the variance between the two sides. For each flow rate, the equation is input into the respective columns, with all values known except for the friction factor. Using Goalseek, the team made the "variance" cell as close to zero as possible by varying the friction factor. With little variance between each side, the equation is virtually equal and the friction factor can be found. The table below outlines the friction factors for each flow rate from 0.5-0.7 lbm/min.

Table 2: Goalseek Data for Colebrook Equation

Flow Rate (lbm/min)	Pressure (psi)	Density (lb_m/ft^3)	Reynolds Number	Relative Roughness	f	Left Side	Right Side	Variance
0.5	38	1.94E-01	28464	0.0015	0.0276	5.480	5.480	6.67E-06
0.5	27	1.38E-01	28464	0.0015	0.0276	5.480	5.480	6.67E-06
0.5	16.5	8.41E-02	28464	0.0015	0.0276	5.480	5.480	6.67E-06
0.55	37.5	1.91E-01	31310	0.0015	0.0272	5.5004	5.5004	4.57E-06
0.55	26.5	1.35E-01	31310	0.0015	0.0272	5.5004	5.5004	4.57E-06
0.55	16	8.15E-02	31310	0.0015	0.0272	5.5004	5.5004	4.57E-06
0.6	36.5	1.86E-01	34157	0.0015	0.0269	5.518	5.5179	9.02E-05
0.6	25.5	1.30E-01	34157	0.0015	0.0269	5.518	5.5179	9.02E-05
0.6	15	7.64E-02	34157	0.0015	0.0269	5.518	5.5179	9.02E-05
0.65	36	1.83E-01	37003	0.0015	0.0266	5.5332	5.5331	8.46E-05
0.65	25	1.27E-01	37003	0.0015	0.0266	5.5332	5.5331	8.46E-05
0.65	15	7.64E-02	37003	0.0015	0.0266	5.5332	5.5331	8.46E-05
0.7	35	1.78E-01	39849	0.0015	0.0264	5.5464	5.5464	5.26E-05
0.7	25	1.27E-01	39849	0.0015	0.0264	5.5464	5.5464	5.26E-05
0.7	14.5	7.39E-02	39849	0.0015	0.0264	5.5464	5.5464	5.26E-05

As can be seen in the table above, as the flow rate increases the friction factor decreases. This is because with more flow and a higher Reynolds number, the force of friction on the flow by the walls of the pipe will have less of an effect on the flow, and will be less of an influence on the pressure drop.

3. The Haaland Equation

   Unlike the Colebrook equation, the Haaland equation can be solved directly and does not require Goalseek to find the friction factor. In this way it is much quicker to use than the Colebrook method [17].

$$\frac{1}{\sqrt{f}} = -1.8\log_{10}\left[\left(\frac{\varepsilon/D}{3.7}\right)^{1.11} + \frac{6.9}{Re}\right] \qquad (4)$$

   The table below outlines the results of using the Haaland equation to find the friction factor.

Table 3: Friction Factor Data for Haaland Equation

Flow Rate (lbm/min)	Pressure (psi)	Density	Reynolds Number	Relative Roughness	f (Haaland)
0.5	38	1.94E-01	28464	0.0015	0.0272
0.5	27	1.38E-01	28464	0.0015	0.0272
0.5	16.5	8.41E-02	28464	0.0015	0.0272
0.55	37.5	1.91E-01	31310	0.0015	0.0269
0.55	26.5	1.35E-01	31310	0.0015	0.0269
0.55	16	8.15E-02	31310	0.0015	0.0269
0.6	36.5	1.86E-01	34157	0.0015	0.0265
0.6	25.5	1.30E-01	34157	0.0015	0.0265
0.6	15	7.64E-02	34157	0.0015	0.0265
0.65	36	1.83E-01	37003	0.0015	0.0263
0.65	25	1.27E-01	37003	0.0015	0.0263
0.65	15	7.64E-02	37003	0.0015	0.0263
0.7	35	1.78E-01	39849	0.0015	0.0260
0.7	25	1.27E-01	39849	0.0015	0.0260
0.7	14.5	7.39E-02	39849	0.0015	0.0260

4. The Swamee-Jain Equation

   Like the Haaland method above, the Swamee-Jain method solves directly for the friction factor. It is also very quick and easy to use [18].

$$f = \frac{0.25}{\left[\log_{10}\left(\frac{\varepsilon}{3.7D} + \frac{5.74}{Re^{0.9}}\right)\right]^2} \qquad (5)$$

The following table outlines the team's results for the Swamee-Jain equation.

Table 4: Friction Factor Data for Swamee-Jain Equation

Flow Rate (lbm/min)	Pressure (psi)	Density	Reynolds Number	Relative Roughness	f (Swamee-Jain)
0.5	38	1.94E-01	28464	0.0015	0.0278
0.5	27	1.38E-01	28464	0.0015	0.0278
0.5	16.5	8.41E-02	28464	0.0015	0.0278
0.55	37.5	1.91E-01	31310	0.0015	0.0274
0.55	26.5	1.35E-01	31310	0.0015	0.0274
0.55	16	8.15E-02	31310	0.0015	0.0274
0.6	36.5	1.86E-01	34157	0.0015	0.0271
0.6	25.5	1.30E-01	34157	0.0015	0.0271
0.6	15	7.64E-02	34157	0.0015	0.0271
0.65	36	1.83E-01	37003	0.0015	0.0268
0.65	25	1.27E-01	37003	0.0015	0.0268
0.65	15	7.64E-02	37003	0.0015	0.0268
0.7	35	1.78E-01	39849	0.0015	0.0266
0.7	25	1.27E-01	39849	0.0015	0.0266
0.7	14.5	7.39E-02	39849	0.0015	0.0266

5. Comparison between all methods

Looking at the results from all of the methods, it is clear that some methods are better for different situations. The figure below is a plot of the friction factor versus the log of the Reynolds number for all of the methods.

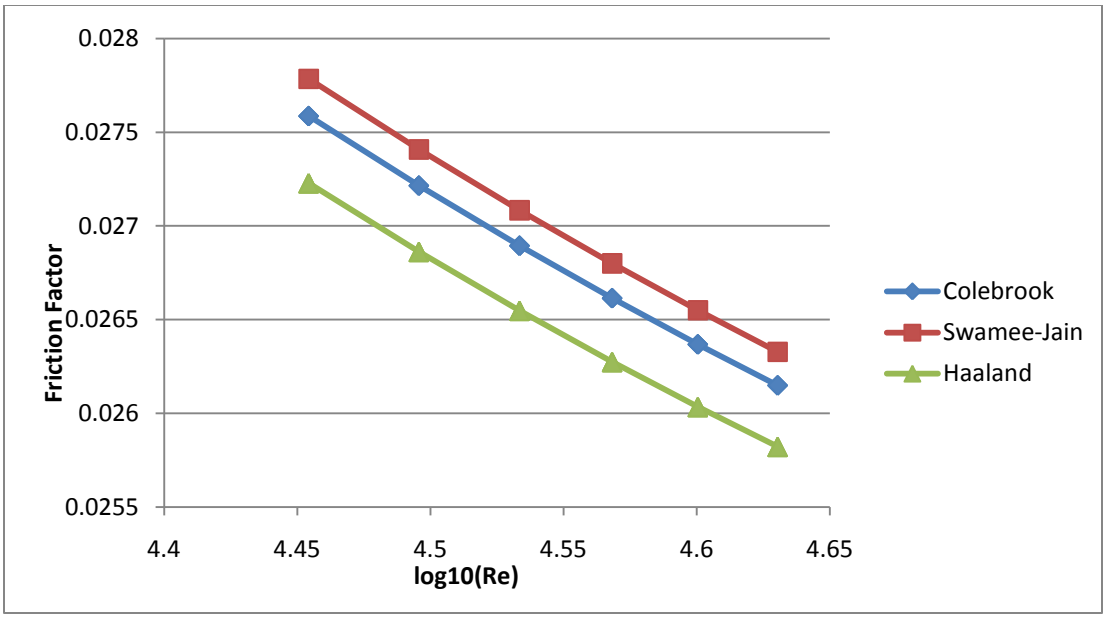

Figure 24: Reynolds Number vs. Friction Factor for Various Calculation Methods

The Moody diagram, the first method used, gave results that were all between 0.026 and 0.027. Since all of the data from the three equations fell in that range, then it is evident that the Moody diagram is a reliable source for finding the friction factor as long as the result does not need to be more accurate. The Moody diagram is by far the quickest method. The Colebrook equation, on the other side of the spectrum, is the longest and most difficult to use. However, it is also the most accurate in finding the friction factor. The Haaland equation gave results that were slightly lower than that of the Colebrook equation, but was still accurate even though it solved directly for the friction factor. The Swamee-Jain method gave results that were roughly 0.005 higher on all points than the Colebrook method. It also solved directly for the friction factor, but is not as accurate as the Haaland equation.

Entry Length

The entry length of the pipe for this system was calculated to be between .22 and .24 meters for the range of this experiment. That is equal to about a foot of pipe. The experiment was built with close to three feet entrance length to be sure the flow would be fully developed before it reached the ten foot length of pipe.

Conclusions

While the mass flow rate was kept constant during the first set of experiments, the volumetric flow rate varied with the pressure due to the changes in gas density. As the gas density decreased, the gas velocity increased through the rotameter which caused the volumetric flow rate to rise. This will be a good phenomenon for students to explain and understand in the unit operations laboratory.

The comparison between the experimental data and the chemical engineering journal article showed that the apparatus constructed by the team accurately attained similar results to the experiment it was modeled off. While the exact data could not be achieved, this was due to the systems inability to simulate such high mass flow rates as were used in the original experiment. The trend shown by the data accurately predicts the same data should the higher mass flow rate have been achieved.

The density is the main value changing in this system to affect the results. This is caused by a change in pressure. A higher pressure makes the fluid denser and slows it down, while a lower pressure makes the fluid less dense and speeds it up. The higher the velocity, the more pressure drop will be present across the pipe. Therefore, as density increases, pressure drop across the pipe decreases.

The COMSOL model showed the same trends as the experimental results. The model had much higher pressure drops across the pipe, and much less difference between pressure jumps. This seems to indicate that the model cannot accurately predict the activity within the pipe. The model can still be used to demonstrate the concepts of pressure drop across a length of pipe. To show a class the trends of pressure drop across a pipe, a professor can use the COMSOL model and it would be easier than taking them to lab to demonstrate.

Recommendations

To further develop the educational purposes of the Unit Operations labs, suggestion are added to improve the quality of the experiment and test other subject matter that are applicable to the apparatus.

2nd pipe

The team would suggest incorporating a second pipe into the system. A different sized pipe would be optimal. This would give the laboratory experiment more time in lab, as well as giving students a comparison between two different sizes of pipe. With two different sized pipes, the students would have a better understanding of how pipe sizing affects turbulence and pressure drop. In addition the use of alternative material which could range from PVC to copper tubing would illustrate the effect of the smoothness of the pipe to pressure drop. The smoother the pipe, the lower of a pressure loss will occur.

Rotameters

As was concluded from the team's calculations between the two rotameters, they are inaccurate with regard to one another. There is no way to tell if one is more accurate than the other since the experimental calculations depend on that information. The team would recommend that two of the same rotameter be used. This would mean either buying another of the first rotameter, or buying two entirely new rotameters. This will be necessary to show students that the following equation is appropriate for calculating the flow rate of the system [2].

$$Q_2 = Q_1 \sqrt{\frac{P_1}{P_2}}$$

Without two rotameters that show the same flowrate, it will not be clear whether or not the square root is necessary in calculating the flow rate.

Anemometers

Anemometers can be found in many of the engineering industries for the measurement of velocity for fluid flow. For the purposes of this project anemometers can be placed at the end of the piping unit for this determination. Despite the use of rotameters in the experiment it was determined a large source of error was present due to the two in use showing significant differences in mass flow rate reading. Using additional equipment will further ensure accurate readings and can be used to calibrate the rotameters. There are multiple types of

anemometers available to sale, but for the purposes of the experiment hot-wire and rotating anemometers will be further discuss.

Heat-wire anemometers utilize a two to three small thin strips of metal, which are located at the end of the device. Due to the small size of the device, it can measure small piping units and other constricted areas. The metal is usually made of platinum, tungsten or an alloy of these components, which is heated to a temperature far above the ambient temperature [12]. Upon the introduction of the gas flowing past the heated metal, the cooling effect of convection is measured. This can be done through measuring the resistance which is dependent upon temperature. The instrument is programmed to determine the wires resistance to the fluid velocity. It is important to note that a constant flow or temperature is necessary for accurate reading in the heat-wire anemometer. These anemometers typically range from 300 to 700 dollars, but can be in excess of a thousand dollars for the higher end models [11]. Despite the advantages to using heat-wire a few problems are also present in these devices. Due to the small and expensive metal which all the measurements are conducted they are easy to break if not handled carefully. Also the supply of gas needs to be free of particulates; otherwise they will accumulate on the wires. While this is not reversible, the wire must be overheated to rid them from the surface.

The alternative anemometer is a rotation based dependent upon the power pressurized gas to move the rotating part, which is recorded to determine the fluid velocity. The two rotating anemometers, windmill and cup abide by the same basic principles but differ in design. This style of equipment was developed far earlier in 1672, with Robert Hooke believed to create the first working model. Price usually ranges from 100 to 300 dollars, and are a much more durable product [8].

Heater

An additional modification to the Pressure Drop Unit Operations experiment is the use of a heater. This tests the student's ability to evaluate the effect of heat to pressure drop in a piping system due to the heats effect upon changes in velocity and air density. From the lab it should be concluded that an increase in temperature of the system will decrease density causing a higher gas velocity. This increased velocity will increase the pressure drop across the ten foot pipe.

There are many different ways to introduce heat into the system; the most effective system would be a T type air process heat. The High Pressure Air (AHP) unit available at omega.com is more than adequate to heat the piping, reaching outlet temperatures of up to 540°C [6]. With the attachment of thermocouples on both sides of the heater will show the temperature rise in the piping. The voltage necessary for outlet air temperatures at to the desired degree can be calculated from the equation below.

$$Watts = SCFM * \emptyset T/3$$

Where:
SCFM is standard cubic feet per minute
ØT is the temperature rise in Fahrenheit from the inlet stream

Based upon the piping equipment limits, flows must range between 2 and 20 CFM, which falls within the specifications of the experiment. The pricing of the heater is relatively inexpensive with prices at or below 100 dollars. In regards to safety the heater could be a potential hazard in the experiment with its high temperature capability, thus placement of controlling features should be considered in the design.

Unit Operations Lab

The following is what the team has put together to give to students in the unit operations laboratory to complete an experiment on the compressible fluid apparatus:

What you need to record in the lab:

- the chosen pressure of the air flowing through the pipes (using the pressure regulator)
- the flow rate through the rotameters (both before and after pressure drop)
- note the temperature of the air above the rotameter for reference
- record the pressure drop across the pipe using the differential pressure gauge

Using the information obtained above you can calculate/verify the following:

- pressure drop across the pipe (in inches of H_2O)
- the mass flow rate calibration value, F_{cal}^{mass}
- the volumetric flow rate in the pipe in SCFM, F_{cal}^{vol}
- the entry length of the pipe, L
- the Reynolds number, Re
- the friction factor in the pipe (a few different ways), f

Before starting the lab, draw a schematic of the apparatus, becoming familiar with the equipment and carefully labeling all valves and meters. List all safety equipment and gear needed to perform the laboratory experiment with explanation. Make a proper procedure detailing the steps needed to complete the experiment(s). Each group should take approximately 5-10 min beforehand and discuss the differences between compressible and incompressible flow. Each group should pick a pressure and pick a mass flow rate to try to calculate what they should be getting for a pressure drop along the given 10 foot section of the pipe. With a mass flow rate in mind, a calculation must be made to determine what volumetric

flow rate must be used at each pressure to achieve that mass flow rate. The equations to calculate this are shown below:

$$F_{actual}^{mass} = F_{cal}^{mass}\sqrt{\frac{P_{actual}}{P_{cal}}}$$

$$F_{cal}^{mass} = F_{cal}^{vol} * \rho_{cal}$$

Where F^{mass}_{actual} is the mass flow rate intended by the lab group, F^{mass}_{cal} is the calibration mass flow rate, P_{actual} is the pressure at the rotameter in psi, P_{cal} is atmospheric pressure in psi, F^{vol}_{cal} is the calibration volumetric flow rate and ρ_{cal} is the density of air at stp (.0746 lb/ft^3).

With the calibration volumetric flow rate determined, the following equation may be used to find the actual volumetric flow rate to set the rotameter to.

$$Q_2 = Q_1\sqrt{\frac{P_1}{P_2}}$$

Where Q_2 is the calibration volumetric flow rate, Q_1 is the actual volumetric flow rate, P_1 is the pressure at the rotameter in psi and P_2 is atmospheric pressure in psi.

Once the lab begins, the group should set the pressure regulator to the calculated pressure and use the manual valve at the end of the experiment to bring the flow rate to what value was decided upon. Once both values match the previously decided values, use the differential pressure gauge to find out the pressure drop. Now compare the calculated value to the experimental value. Are they the same? Why or Why not? If not, give some possible explanations to why this could be.

Look in the calculation references section below about the friction factor. After solving all the given equations for the friction factor, give some pros and cons for each of the given equations and recommend which one of the equations you would use.

Calculation References:

Students in the lab would also be given the following equations to use in their calculations in the lab.

The entry length is the length of pipe necessary for the internal flow to become a fully developed flow. Using the following equation, the entry length was calculated:

$$L = \frac{2\Delta P D}{\rho f_{darcy} V^2}$$

Where the ΔP is the pressure drop across the pipe in pascals, the D is the diameter of the pipe in meters, the ρ is the density of the air in kg/m^3, the V is the velocity of the air in m/s, and the f_{darcy} is the darcy friction factor.

The pressure drop across the pipe will change when the flow rate of air and the pressure of the air are varied. The differential pressure gauge will give the value in lbs/in^2, so to convert that to inches of water you do the following:

$$\Delta P = \Delta P_{psi} \times \frac{27.7\ inches\ of\ H_20}{1\ psi}$$

The Darcy friction factor is a dimensionless quantity that factors for friction losses as the fluid flows through a pipe. This factor relies on both the Reynolds number of the flow and the inside diameter of the pipe. The Darcy friction factor can be calculated using several methods, as follows:

Colebrook Equation:

$$\frac{1}{\sqrt{f}} = -2\log_{10}\left(\frac{\varepsilon/D}{3.7} + \frac{2.51}{Re\sqrt{f}}\right)$$

Haaland Equation:

$$\frac{1}{\sqrt{f}} = -1.8\log_{10}\left[\left(\frac{\varepsilon/D}{3.7}\right)^{1.11} + \frac{6.9}{Re}\right]$$

Swamee-Jain Equation:

$$f = \frac{0.25}{\left[\log_{10}\left(\frac{\varepsilon}{3.7D} + \frac{5.74}{Re^{0.9}}\right)\right]^2}$$

Where f is the Darcy friction factor (dimensionless), ε is the Roughness height of the pipe in feet, D is the diameter of the pipe in feet, and Re is the Reynolds number (dimensionless).

The Reynolds number is the ratio of the inertial forces to the viscous forces and is used as a measure to determine the type of flow inside the pipe. The equation used to calculate the Reynolds number is:

$$Re = \frac{\rho \times V \times D}{\mu \times g_c}$$

Where the ρ is the density of the gas in lb_m/ft^3, the V is the velocity in ft/sec, the D is the diameter in feet, the μ is the dynamic viscosity in lb_f*s/ft^2, and the g_c is the gravity constant at 32.17 $lb_f ft/lb_m sec^2$.

The mass flow rate calibration value is used to find the calibration volumetric flow rate in the pipe. The equation for the mass flow rate calibration value is:

$$F_{cal} = \frac{Mass\ Flow\ Rate\ actual}{\sqrt{\frac{P_{actual}}{P_{cal}}}}$$

Where the actual mass flow rate is the value assumed by the lab group, P_{actual} is the actual pressure in psia, and the P_{cal} is the calibration pressure which is at ambient room pressure, or 14.7 psia.

The volumetric flow rate is calculated from the mass flow rate calibration value above over the calibration density of the air, which in this case is 0.746.

$$Volumetric\ Flowrate\ (SCFM) = \frac{F_{cal}}{\rho_{cal}}$$

References

1. Luyben, William L., and Kemal Tuzla. "Gas Pressure-Drop Experiment." *Chemical Engineering Education* 44.3 (2010): 183-88. Print.

2. Fox, Robert W., Alan T. McDonald, and Philip J. Pritchard. *Introduction to Fluid Mechanics*. 7th ed. Hoboken, NJ: Wiley, 2009. Print.

3. Moody diagram: http://people.msoe.edu/tritt/be382/MoodyChart.html

4. McCabe, Warren L., Julian C. Smith, and Peter Harriott. *Unit Operations of Chemical Engineering*. 7th ed. Boston: McGraw-Hill, 2005. Print.

5. www.COMSOL.com

6. *Omega.com*. Omega Engineering Inc. Web. 29 Mar. 2011.

7. "Dwyer Instruments Online Catalog." *Dwyer Instruments Online*. Web. 07 Nov. 2010. <http://catalogs.dwyer-inst.com/WebProject.asp?CodeId=7.4.2.2>.

8. "Grainger Industrial Supply." Grainger Industrial Supply - MRO Supplies, MRO Equipment, Tools & Solutions. Web. 10 Nov. 2010. <http://www.grainger.com/Grainger/wwg/viewCatalogPDF>.

9. Abel, Alan, Phil Lowe, Rachel Clair, and Daqian Wu. "Compressible Fluid Flow: Pressurizing and Discharging of Tanks Under Adiabatic and Isothermal Conditions." Carnegie Mellon University, 22 May 2006. Web. 24 Mar. 2011. <http://rothfus.cheme.cmu.edu/tlab/compflow/projects/t6s06/t6_s06_r3.pdf>.

10. Dutton, J. Craig, and Robert E. Coverdill. "Experiments to Study the Gaseous Discharge and Filling of Vessels." *International Journal of Engineering Education* 13.2 (1997): 123-34. TEMPUS Publications, 1997. Web. 23 Mar. 2011. <http://www.akademik.unsri.ac.id/download/journal/files/ijee/ijee924.pdf>.

11. "Hot Wire Anemometers: Introduction." *Efunda.com*. 2011. Web. 18 Mar. 2011. <http://www.efunda.com/designstandards/sensors/hot_wires/hot_wires_intro.cfm>.

12. "Hot Wire Anemometry." *Annual Review of Fluid Mechanics* 8 (1976): 209-31.*Annualreviews.org*. Web of Science. Web. 25 Mar. 2011. <http://www.annualreviews.org/doi/pdf/10.1146/annurev.fl.08.010176.001233>.

13. "Pipe Flow 3D - Pressure Drop Theory." *Pipeflow.co.uk*. Daxesoft Ltd. Web. 29 Mar. 2011. <http://pipeflow.co.uk/public/control.php?_path=/417/503/510>.

14. Smith, J. M., H. C. Van Ness, and Michael M. Abbott. *Introduction to Chemical Engineering Thermodynamics*. 7th ed. Boston: McGraw-Hill, 2005. Print.

15. "Fluid Pressure Drop Along Pipe Length of Uniform Diameter." *Engineersedge.com*. Engineers Edge. Web. 1 Apr. 2011. <Engineersedge.com/fluid_flow/pressure_drop/pressure_drop.htm>.

16. Colebrook: Colebrook, C.F. (February 1939). "Turbulent flow in pipes, with particular reference to the transition region between smooth and rough pipe laws". *Journal of the Institution of Civil Engineers* (London).

17. Haaland: Haaland, S.E., 1983. Simple and explicit formulas for the friction factor in turbulent pipe flow. *J. Fluids Eng.*

18. Swamee-Jain: Swamee, PK (1976). "Explicit equations for pipe-flow problems". Journal of the Hydraulics Division (0044-796X), 102 (5), p. 657.

Appendix

ρcal	0.0746	Works for all experiments because it is the calibration value, not the calculated value								
Area	0.000706858									
Flow Rate	Pressure (psi)	F cal		P2	Fvol reading	P at vol 2	Fvol reading 2	Fvol Actual	Delta P (psi)	Delta P (in H2O)
0.5	40	0.2592	38	38	3.386553834	1.75	7	3.474530922	0.8	22.16
0.5	30	0.286731	27	27	3.646341476	1.5	6.7	3.843581397	0.85	23.545
0.5	20	0.325435	16.5	16.5	3.962343124	1.4	6.5	4.362396205	0.95	26.315
0.55	40	0.28512	37.5	37.5	3.700620109	2.1	7.5	3.821984014	0.85	23.545
0.55	30	0.315404	26.5	26.5	3.973663411	1.9	7.2	4.227939536	0.9	24.93
0.55	20	0.357978	16	16	4.292030362	1.6	6.8	4.798635825	1.05	29.085
0.6	40	0.31104	36.5	36.5	3.982849203			4.169437106	0.95	26.315
0.6	30	0.344077	25.5	25.5	4.252328347	2.25	7.8	4.612297676	1.05	29.085
0.6	20	0.390522	15	15	4.533535122			5.234875446	1.15	31.855
0.65	40	0.33696	36	36	4.284253774			4.516	1.05	29.085
0.65	30	0.372751	25	25	4.561616033	2.4	8	4.997	1.15	31.855
0.65	20	0.423065	15	15	4.911230065			5.671	1.3	36.01
0.7	40	0.36288	35	35	4.550176501			4.864343291	1.15	31.855
0.7	30	0.401424	25	25	4.912171209			5.381013955	1.3	36.01
0.7	20	0.455609	14.5	14.5	5.200225132			6.107354687	1.45	40.165
0.75	40	0.3888	30	30	4.513724405			5.212	1.35	37.395
0.75	30	0.430097	24.5	24.5	5.209808098			5.765	1.45	40.165
0.75	20	0.488152	14	14	5.475103214			6.544	1.65	45.705
0.85	40	0.44064						5.906702567		0
0.85	30	0.487443						6.534088374	2.05	56.785
0.85	20	0.553239						7.416073548		0
0.95	40	0.49248						6.601608752		0
0.95	30	0.544789						7.302804653		0
0.95	20	0.618326						8.288552789		0

Velocity (m/s)	COMSOL P (Pa)	COMSOL Delta P (Pa)	Delta P exp (Pa)	COMSOL Delta P (in H2O)	sqrt of pressures		
26.87265362	363272	6700	5520	26.89782	40 psi	1.929012	
29.72695706	287438	6800	5865	27.29928	30 psi	1.743794	
33.73956508	215051	6900	6555	27.70074	20 psi	1.536406	
29.55991898	359825	8000	5865	32.1168			
32.69965277	283991	8000	6210	32.1168			
37.11352159	211604	8000	7245	32.1168			
32.24718434	352931	9100	6555	36.53286			
35.67234847	277097	9200	7245	36.93432			
40.48747809	204710	9300	7935	37.33578			
34.92756475	349484	10600	7245	42.55476			
38.64770617	273650	10700	7935	42.95622			
43.86054466	204710	10800	8970	43.35768			
37.62171507	342590	12100	7935	48.57666			
41.61773989	273650	12400	8970	49.78104			
47.23539111	201263	13400	10005	53.79564			
40.31055524	308120	12700	9315	50.98542			
44.58755774	270203	14000	10005	56.2044			
50.61248532	197816	14100	11385	56.60586			

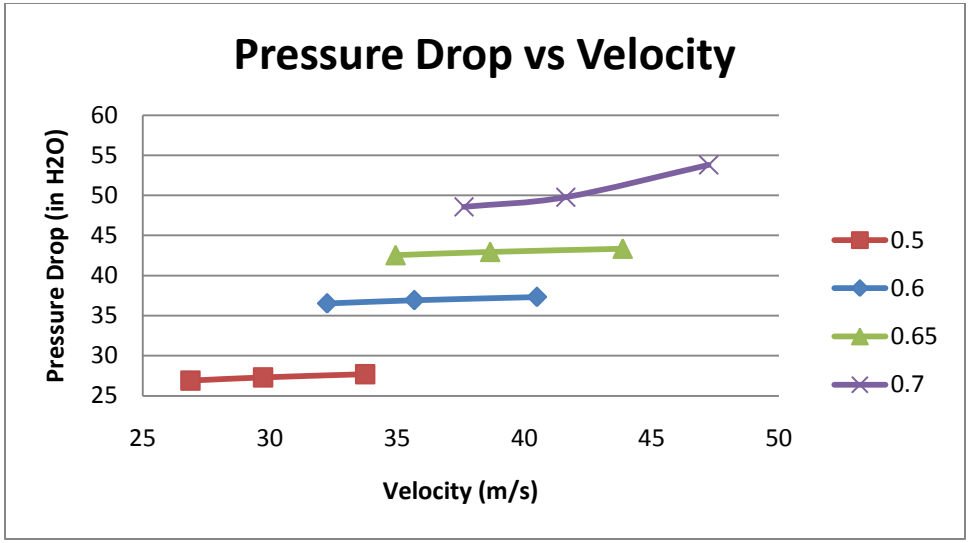
Pressure Drop vs Velocity
Pressure Drop (in H2O)
60
55
50
45
40
35
30
25
25
30
35
40
45
50
Velocity (m/s)
0.5
0.6
0.65
0.7

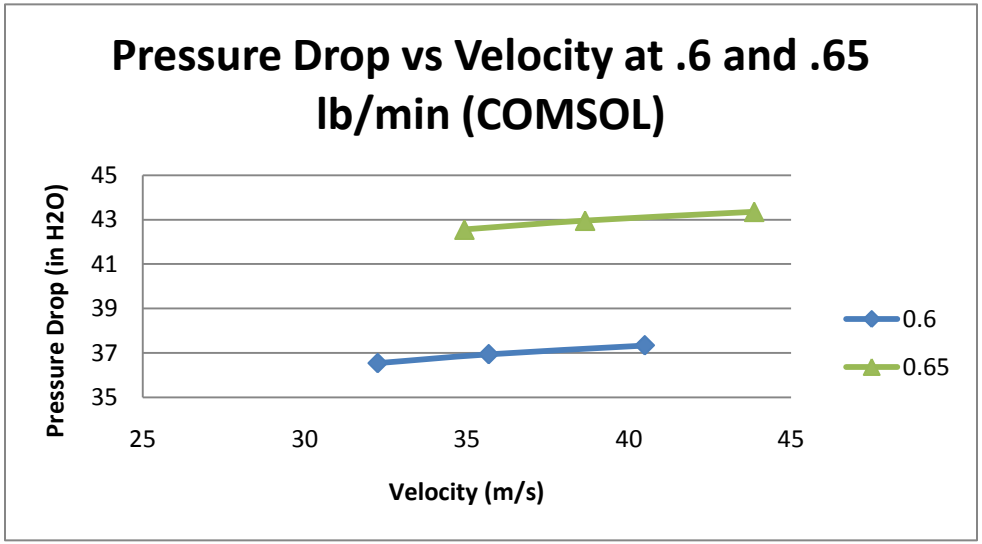
Pressure Drop vs Velocity at .6 and .65 lb/min (COMSOL)
Pressure Drop (in H2O)
45
43
41
39
37
35
25
30
35
40
45
Velocity (m/s)
0.6
0.65

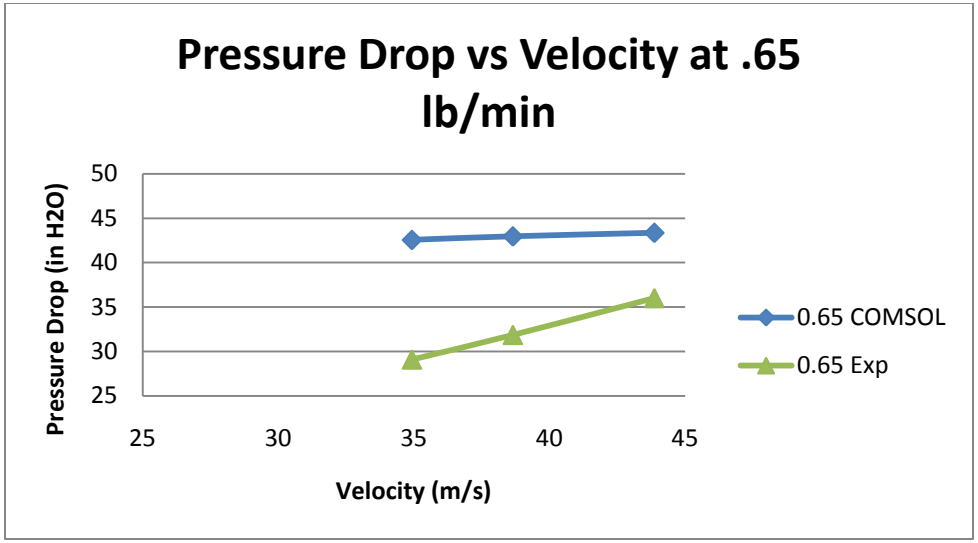
Pressure Drop vs Velocity at .65 lb/min
Pressure Drop (in H2O)
50
45
40
35
30
25
25
30
35
40
45
Velocity (m/s)
0.65 COMSOL
0.65 Exp

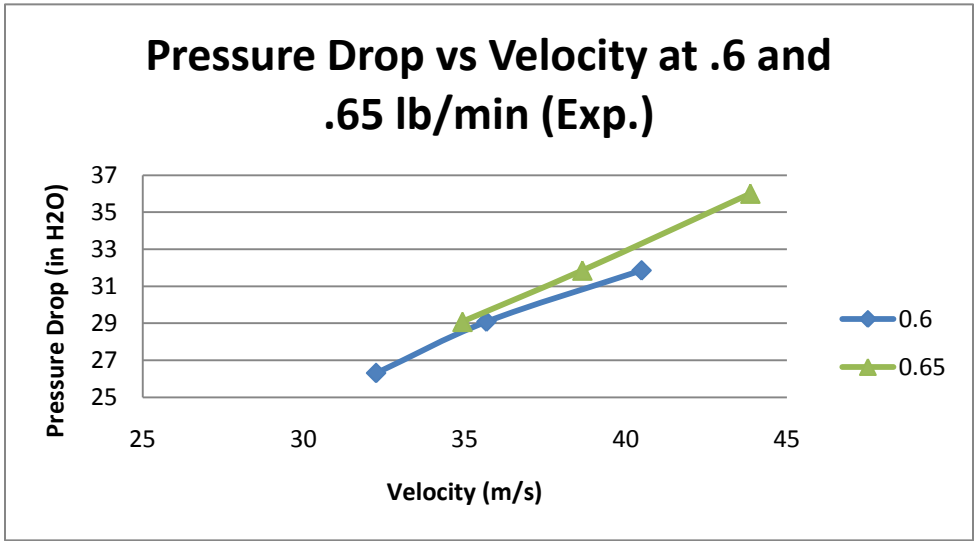
Pressure Drop vs Velocity at .6 and .65 lb/min (Exp.)
Pressure Drop (in H2O)
37
35
33
31
29
27
25
25
30
35
40
45
Velocity (m/s)
0.6
0.65

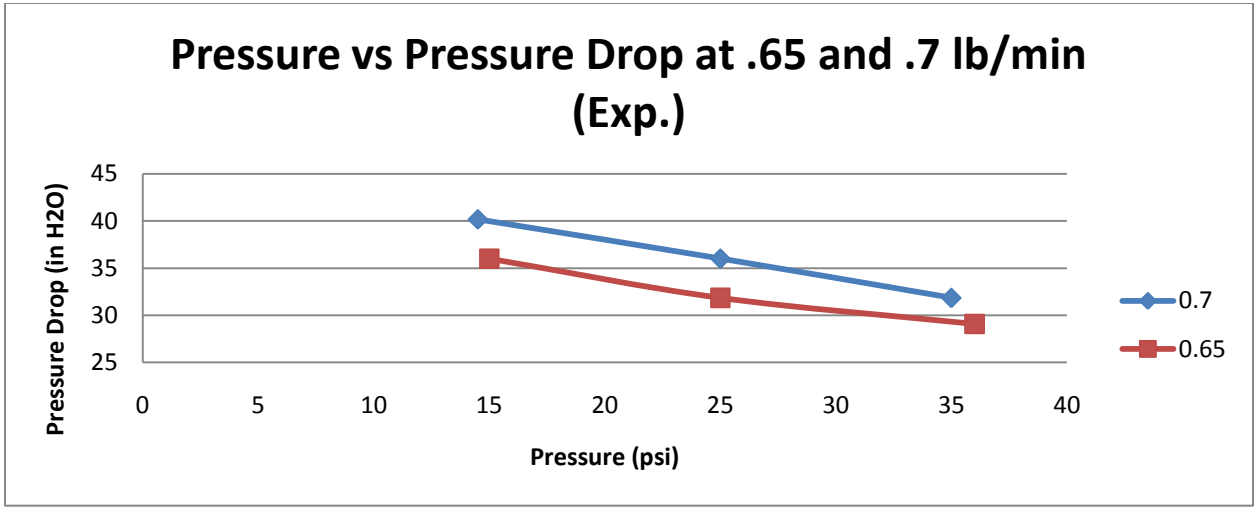
Pressure vs Pressure Drop at .65 and .7 lb/min (Exp.)
Pressure Drop (in H2O)
45
40
35
30
25
0
5
10
15
20
25
30
35
40
Pressure (psi)
0.7
0.65

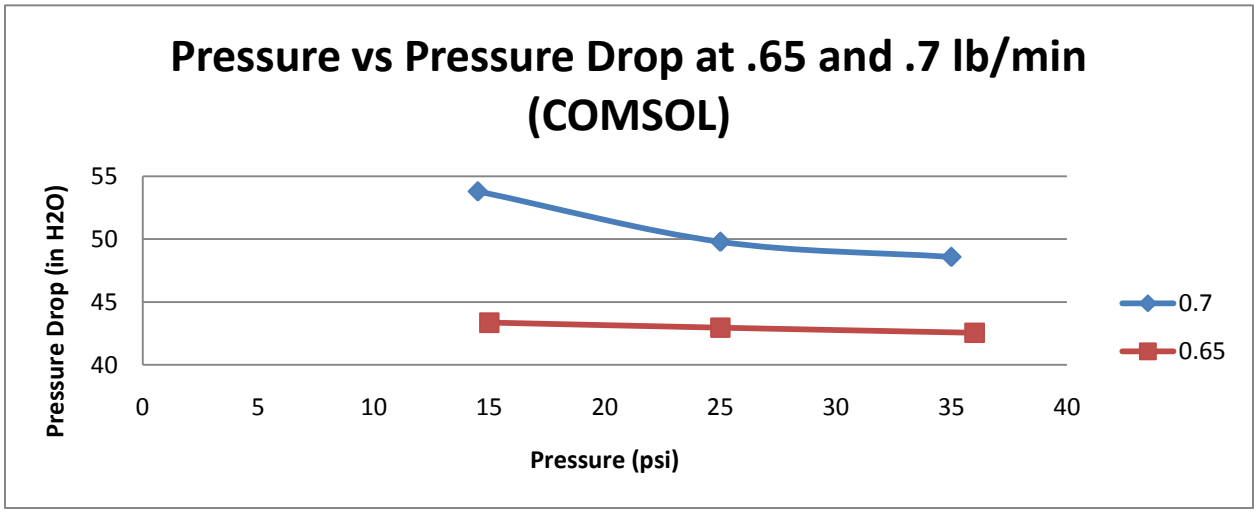
Pressure vs Pressure Drop at .65 and .7 lb/min (COMSOL)
Pressure Drop (in H2O)
55
50
45
40
0
5
10
15
20
25
30
35
40
Pressure (psi)
0.7
0.65

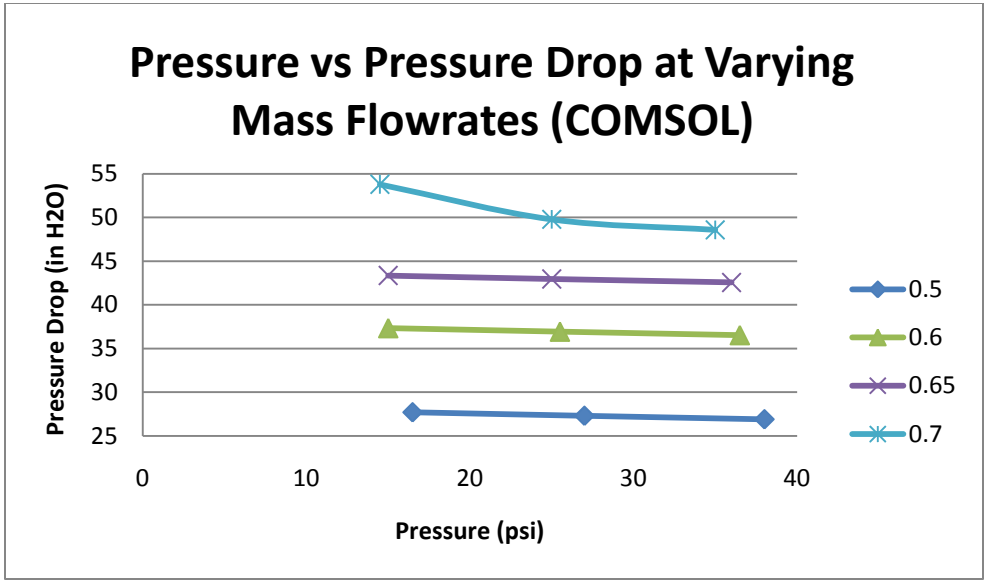
Pressure vs Pressure Drop at Varying Mass Flowrates (COMSOL)
Pressure Drop (in H2O)
55
50
45
40
35
30
25
0
10
20
30
40
Pressure (psi)
0.5
0.6
0.65
0.7

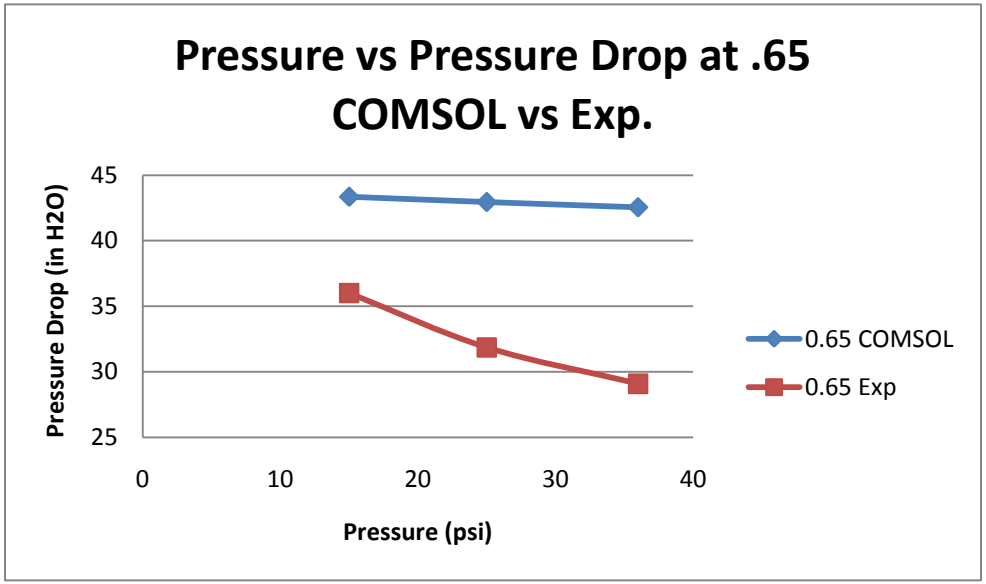
Pressure vs Pressure Drop at .65 COMSOL vs Exp.
Pressure Drop (in H2O)
45
40
35
30
25
0
10
20
30
40
Pressure (psi)
0.65 COMSOL
0.65 Exp

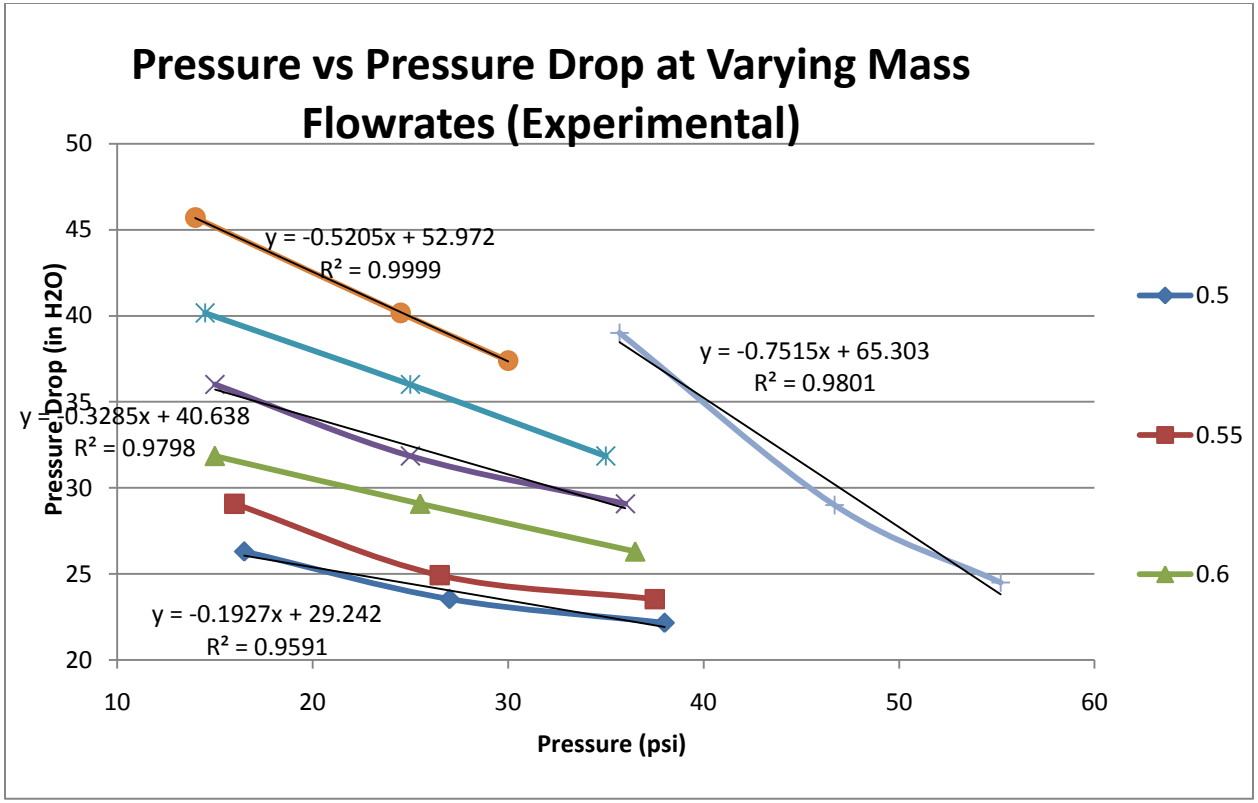
Pressure vs Pressure Drop at Varying Mass Flowrates (Experimental)
Pressure Drop (in H2O)
Pressure (psi)
50
45
40
35
30
25
20
10
20
30
40
50
60
y = -0.5205x + 52.972
R² = 0.9999
y = -0.7515x + 65.303
R² = 0.9801
y = -0.3285x + 40.638
R² = 0.9798
y = -0.1927x + 29.242
R² = 0.9591
0.5
0.55
0.6

Density (lbm/ft^3)	Pressure	Flow Rate (lbm/min)	Velocity (ft/sec)	Diameter (in)	Diameter (ft)	Area (in^2)	Area (ft^2)	Dynamic Viscosity (lbf*s/ft^2)	Kinematic Viscosity (ft^2/s)	Reynolds number	log10(Re)	roughness e (ft)
0.193634	38	0.5	59.5535	0.364	0.030333	0.104062	0.000723	3.82E-07	6.35E-05	2.85E+04	4.454294	4.92E-05
0.137582	27	0.5	83.81604	0.364	0.030333	0.104062	0.000723	3.82E-07	8.93E-05	28463.89	4.454294	4.92E-05
0.084078	16.5	0.5	137.1535	0.364	0.030333	0.104062	0.000723	3.82E-07	1.46E-04	28463.89	4.454294	4.92E-05
0.191086	37.5	0.55	66.3823	0.364	0.030333	0.104062	0.000723	3.82E-07	6.43E-05	31310.28	4.495687	4.92E-05
0.135034	26.5	0.55	93.93722	0.364	0.030333	0.104062	0.000723	3.82E-07	9.10E-05	31310.28	4.495687	4.92E-05
0.08153	16	0.55	155.5835	0.364	0.030333	0.104062	0.000723	3.82E-07	1.51E-04	31310.28	4.495687	4.92E-05
0.18599	36.5	0.6	74.40109	0.364	0.030333	0.104062	0.000723	3.82E-07	6.61E-05	34156.67	4.533476	4.92E-05
0.129939	25.5	0.6	106.4957	0.364	0.030333	0.104062	0.000723	3.82E-07	9.46E-05	34156.67	4.533476	4.92E-05
0.076434	15	0.6	181.0426	0.364	0.030333	0.104062	0.000723	3.82E-07	1.61E-04	34156.67	4.533476	4.92E-05
0.183443	36	0.65	81.72064	0.364	0.030333	0.104062	0.000723	3.82E-07	6.70E-05	37003.06	4.568238	4.92E-05
0.127391	25	0.65	117.6777	0.364	0.030333	0.104062	0.000723	3.82E-07	9.65E-05	37003.06	4.568238	4.92E-05
0.076434	15	0.65	196.1295	0.364	0.030333	0.104062	0.000723	3.82E-07	1.61E-04	37003.06	4.568238	4.92E-05
0.178347	35	0.7	90.52132	0.364	0.030333	0.104062	0.000723	3.82E-07	6.89E-05	39849.45	4.600422	4.92E-05
0.127391	25	0.7	126.7299	0.364	0.030333	0.104062	0.000723	3.82E-07	9.65E-05	39849.45	4.600422	4.92E-05
0.073887	14.5	0.7	218.4997	0.364	0.030333	0.104062	0.000723	3.82E-07	1.66E-04	39849.45	4.600422	4.92E-05
0.152869	30	0.75	113.1517	0.364	0.030333	0.104062	0.000723	3.82E-07	8.04E-05	42695.84	4.630386	4.92E-05
0.124843	24.5	0.75	138.553	0.364	0.030333	0.104062	0.000723	3.82E-07	9.84E-05	42695.84	4.630386	4.92E-05
0.071339	14	0.75	242.4678	0.364	0.030333	0.104062	0.000723	3.82E-07	1.72E-04	42695.84	4.630386	4.92E-05
0.278731	55.2	0.83	68.67705	0.364	0.030333	0.104062	0.000723	3.82E-07	4.41E-05	47250.06	4.674402	4.92E-05
0.235418	46.7	0.83	81.31244	0.364	0.030333	0.104062	0.000723	3.82E-07	5.22E-05	47250.06	4.674402	4.92E-05
0.178092	35.7	0.83	107.486	0.364	0.030333	0.104062	0.000723	3.82E-07	6.90E-05	47250.06	4.674402	4.92E-05

relative roughness	darcy friction factor using Colebrook iterations	darcy friction factor using Swamee–Jain equation	darcy friction factor using Haaland equation	Predicted Pressure Drop using formula from document lbm/fts^2	in inches water	Entry Leng
0.001622	0.027586973	0.027784909	0.027228154	3122.840611	18.64369	0.221247
0.001622	0.027586973	0.027784909	0.027228154	4395.109008	26.23926	0.221247
0.001622	0.027586973	0.027784909	0.027228154	7191.996559	42.93698	0.224789
0.001622	0.027215416	0.027408297	0.026862088	3777.447456	22.55176	0.224789
0.001622	0.027215416	0.027408297	0.026862088	5345.444513	31.91287	0.224789
0.001622	0.027215416	0.027408297	0.026862088	8853.392475	52.85568	0.228073
0.001622	0.026894796	0.027083468	0.026547613	4564.227142	27.24892	0.228073
0.001622	0.026894796	0.027083468	0.026547613	6533.109439	39.00335	0.228073
0.001622	0.026894796	0.027083468	0.026547613	11106.28605	66.3057	0.231136
0.001622	0.02661498	0.02680002	0.026274282	5374.520336	32.08645	0.231136
0.001622	0.02661498	0.02680002	0.026274282	7739.309284	46.20449	0.231136
0.001622	0.02661498	0.02680002	0.026274282	12898.84881	77.00748	0.234008
0.001622	0.02636841	0.026550226	0.026034336	6351.866134	37.92131	0.234008
0.001622	0.02636841	0.026550226	0.026034336	8892.612588	53.08983	0.234008
0.001622	0.02636841	0.026550226	0.026034336	15332.09067	91.53419	0.236715
0.001622	0.026149327	0.026328209	0.025821885	8436.283007	50.3655	
0.001622	0.026149327	0.026328209	0.025821885	10330.14246	61.67204	
0.001622	0.026149327	0.026328209	0.025821885	18077.7493	107.9261	
0.001622	0.025781799	0.026019764	0.02552814	5028.216049	30.01898	
0.001622	0.025781799	0.026019764	0.02552814	5953.320734	35.54195	
0.001622	0.025781799	0.026019764	0.02552814	7869.625691	46.98249	

darcy factor iterations (goalseek)

Flow Rate (lbm/min)		f	Left Side	Right Side	Variance
0.5		0.0276	6.0207	6.0270	-6.28E-03
0.55		0.0272	6.0617	6.0683	-6.59E-03
0.6		0.0269	6.0977	6.1046	-6.87E-03
0.65		0.0266	6.1297	6.1368	-7.14E-03
0.7		0.0264	6.1583	6.1656	-7.39E-03
0.75		0.0261	6.1840	6.1916	-7.62E-03
0.83		0.0258	6.2279	6.2278	1.42E-04

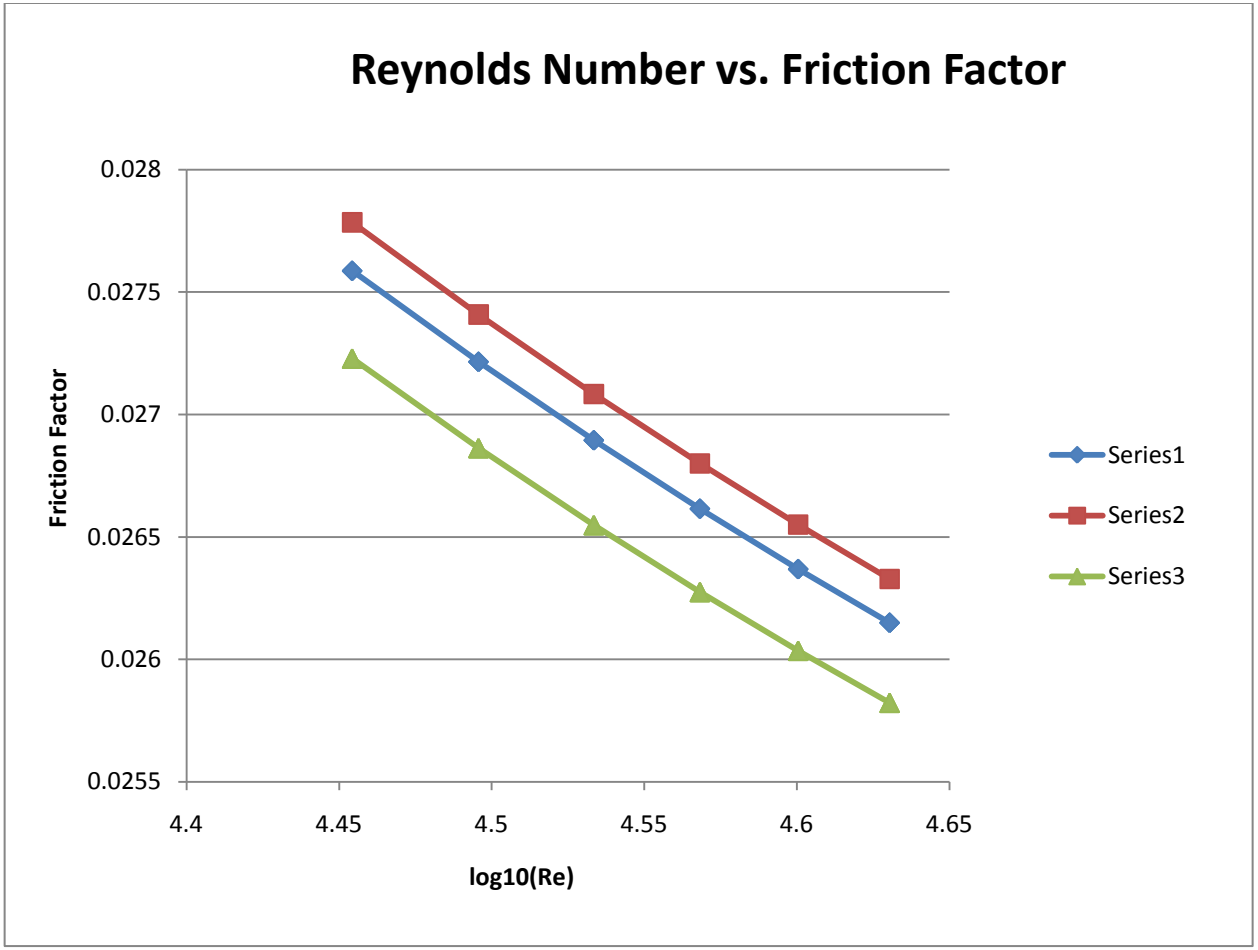
Reynolds Number vs. Friction Factor
0.028
0.0275
0.027
0.0265
0.026
0.0255
Friction Factor
4.4
4.45
4.5
4.55
4.6
4.65
log10(Re)
Series1
Series2
Series3

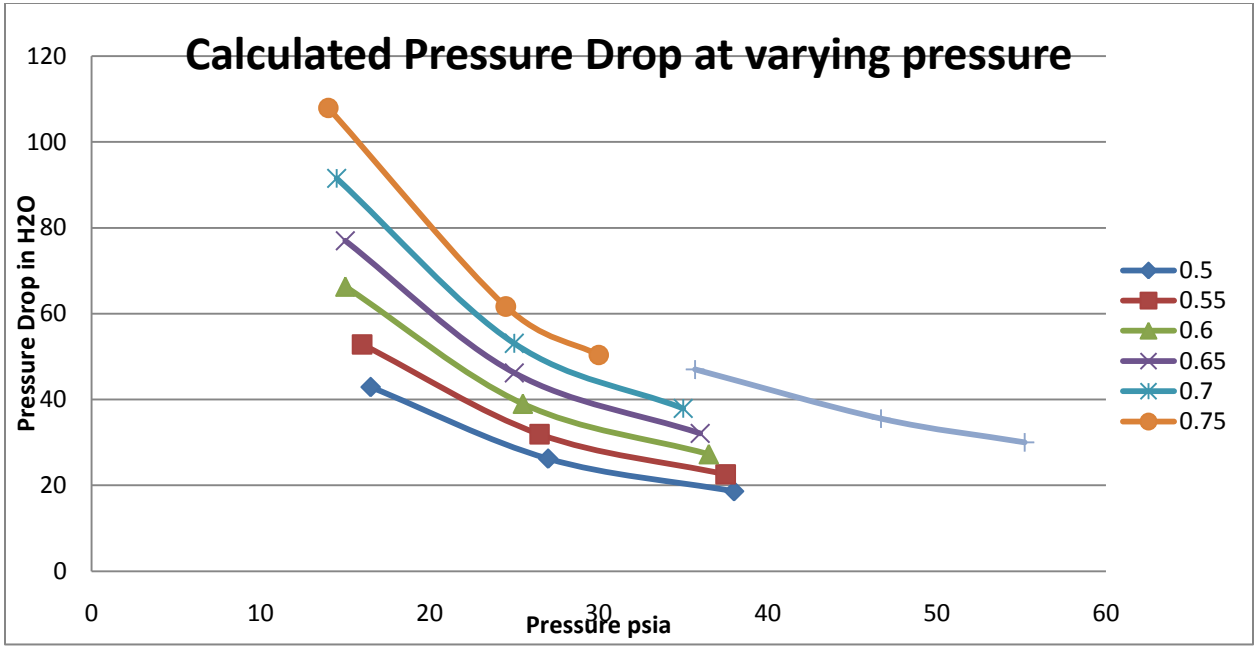
Calculated Pressure Drop at varying pressure
Pressure Drop in H2O
120
100
80
60
40
20
0
0
10
20
30
40
50
60
Pressure psia
0.5
0.55
0.6
0.65
0.7
0.75

psia	P (psi)	P (pa)	T (K)	R (Pa*m^3/K*mol)	MW (g/mol)	Density (kg/m^3)	Density (lb/ft^3)		
38	38	261972	294.26	8.314	28.966	3.101716863	0.193633858		
27	27	186138	294.26	8.314	28.966	2.203851456	0.137581952		
16.5	16.5	113751	294.26	8.314	28.966	1.346798112	0.084077859		
37.5	37.5	258525	294.26	8.314	28.966	3.060904799	0.191086044		
26.5	26.5	182691	294.26	8.314	28.966	2.163039392	0.135034138		
16	16	110304	294.26	8.314	28.966	1.305986048	0.081530046		
36.5	36.5	251631	294.26	8.314	28.966	2.979280671	0.185990416		
25.5	25.5	175797	294.26	8.314	28.966	2.081415264	0.12993851		
15	15	103410	294.26	8.314	28.966	1.22436192	0.076434418		
36	36	248184	294.26	8.314	28.966	2.938468607	0.183442602		
25	25	172350	294.26	8.314	28.966	2.0406032	0.127390696		
15	15	103410	294.26	8.314	28.966	1.22436192	0.076434418		
35	35	241290	294.26	8.314	28.966	2.856844479	0.178346975		
25	25	172350	294.26	8.314	28.966	2.0406032	0.127390696		
14.5	14.5	99963	294.26	8.314	28.966	1.183549856	0.073886604		
30	30	206820	294.26	8.314	28.966	2.44872384	0.152868835		
24.5	24.5	168903	294.26	8.314	28.966	1.999791136	0.124842882		
14	14	96516	294.26	8.314	28.966	1.142737792	0.07133879		
54.7	40	377101.8	294.26	8.314	28.966	4.464839801	0.278730843		
46.2	31.5	318502.8	294.26	8.314	28.966	3.771034713	0.235418006		
34.95	20.25	240945.3	294.26	8.314	28.966	2.852763273	0.178092193		

COMSOL Model Report

1. Table of Contents

2. Model Properties

Property	Value
Model name	
Author	
Company	
Department	
Reference	
URL	
Saved date	Apr 26, 2011 4:01:32 PM
Creation date	Jan 20, 2011 3:54:48 PM
COMSOL version	COMSOL 3.5.0.608

File name: R:\MQP Turbulent quarter inch part 3.mph

Application modes and modules used in this model:

- Geom1 (Axial symmetry (2D))

- k-ε Turbulence Model (Chemical Engineering Module)

3. Constants

Name	Expression	Value	Description
T	298		
P	92514		

4. Geometry

Number of geometries: 1

4.1. Geom1

4.1.1. Point mode

4.1.2. Boundary mode

4.1.3. Subdomain mode

5. Geom1

Space dimensions: Axial symmetry (2D)

Independent variables: r, phi, z

5.1. Mesh

5.1.1. Mesh Statistics

Number of degrees of freedom	26200
Number of mesh points	1804

Number of elements	2492
Triangular	2492
Quadrilateral	0
Number of boundary elements	1114
Number of vertex elements	4
Minimum element quality	0.172
Element area ratio	0

5.2. Application Mode: k-ε Turbulence Model (chns)

Application mode type: k-ε Turbulence Model (Chemical Engineering Module)

Application mode name: chns

5.2.1. Scalar Variables

Name	Variable	Value	Unit	Description
visc_vel_fact	visc_vel_fact_chns	10	1	Viscous velocity factor
Cd1	Cd1_chns	1.44	1	C,ε1 turbulence modeling constant
Cd2	Cd2_chns	1.92	1	C,ε2 turbulence modeling constant
sigmak	sigmak_chns	1.0	1	σ,k turbulence modeling constant
sigmad	sigmad_chns	1.3	1	σ,ε turbulence modeling constant
Cmu	Cmu_chns	0.09	1	C,μ turbulence modeling constant
Cplus	Cplus_chns	5.5	1	Logarithmic wall function constant
kappa	kappa_chns	0.42	1	κ von Karman constant

5.2.2. Application Mode Properties

Property	**Value**

Default element type	Lagrange - P_2 P_1
Analysis type	Stationary
Corner smoothing	Off
Weakly compressible flow	On
Turbulence model	k-ε
Realizability	Off
Non-Newtonian flow	Off
Brinkman on by default	Off
Two-phase flow	Single-phase flow
Swirl velocity	Off
Frame	Frame (ref)
Weak constraints	Off
Constraint type	Ideal

5.2.3. Variables

Dependent variables: u, v, w, p, logk, logd, logw, phi, psi, nrw, nzw

Shape functions: shlag(2,'u'), shlag(2,'v'), shlag(1,'p'), shlag(2,'logk'), shlag(2,'logd')

Interior boundaries not active

5.2.4. Boundary Settings

Boundary		1	2	3
Type		Symmetry boundary	Inlet	Outlet
symtype		**Axial symmetry**	Symmetry	Symmetry
Pressure (p0)	Pa	0	0	**363272**
Normal inflow velocity (U0in)	m/s	1	**26.87**	1
Normal outflow velocity (U0out)	m/s	0	0	**53**

Boundary		4
Type		Wall
symtype		Symmetry
Pressure (p0)	Pa	0
Normal inflow velocity (U0in)	m/s	1
Normal outflow velocity (U0out)	m/s	0

5.2.5. Subdomain Settings

Subdomain		1
Integration order (gporder)		**4 4 2 4 4**
Constraint order (cporder)		**2 2 1 2 2**
Density (rho)	kg/m^3	**rho(p[1/Pa],T[1/K])[kg/m^3] (Air)**
Dynamic viscosity (eta)	Pa·s	**eta(T[1/K])[Pa*s] (Air)**
Surface tension coefficient (sigma)	N/m	**0[S/m] (Air)**
Reinitialization parameter (gamma)	m/s	**1.4 (Air)**

Subdomain initial value		1
Logarithm of turbulent kinetic energy (logk)	1	101325

6. Materials/Coefficients Library

6.1. Air

Parameter	**Value**
Heat capacity at constant pressure (C)	Cp(T[1/K])[J/(kg*K)]
Speed of sound (cs)	cs(T[1/K])[m/s]
Dynamic viscosity (eta)	eta(T[1/K])[Pa*s]
Ratio of specific heats (gamma)	1.4

Thermal conductivity (k)	k(T[1/K])[W/(m*K)]
Kinematic viscosity (nu0)	nu0(T[1/K])[m^2/s]
Density (rho)	rho(p[1/Pa],T[1/K])[kg/m^3]
Electric conductivity (sigma)	0[S/m]

6.1.1. Functions

Function	Expression	Derivatives	Complex output
cs(T)	sqrt(1.4*287*T)	d(sqrt(1.4*287*T),T)	false
rho(p,T)	p*0.02897/8.314/T	d(p*0.02897/8.314/T,p), d(p*0.02897/8.314/T,T)	false

6.1.2. Piecewise Analytic Functions

6.1.2.1. Function: Cp(T)

Type: Polynomial

x_{start}	x_{end}	f(x)
200	1600	0 1.04763657E+03 1 -3.72589265E-01 2 9.45304214E-04 3 -6.02409443E-07 4 1.28589610E-10

6.1.2.2. Function: eta(T)

Type: Polynomial

x_{start}	x_{end}	f(x)
200	1600	0 -8.38278000E-07 1 8.35717342E-08 2 -7.69429583E-11 3 4.64372660E-14 4 -1.06585607E-17

6.1.2.3. Function: nu0(T)

Type: Polynomial

x_{start}	x_{end}	f(x)
200	1600	0 -5.86912450E-06 1 5.01274491E-08 2 7.50108343E-11 3 1.80336823E-15 4 -2.91688030E-18

6.1.2.4. Function: k(T)

Type: Polynomial

x_{start}	x_{end}	f(x)
200	1600	0 -2.27583562E-03 1 1.15480022E-04 2 -7.90252856E-08 3 4.11702505E-11 4 -7.43864331E-15

7. Solver Settings

Solve using a script: off

Analysis type	Stationary
Auto select solver	On
Solver	Stationary segregated
Solution form	Automatic
Symmetric	Off
Adaptive mesh refinement	Off
Optimization/Sensitivity	Off
Plot while solving	Off

7.1. Segregated Groups

7.1.1. Group 1

Parameter	Value
Components	u v p
Tolerance	1e-3

7.1.1.1. Direct (PARDISO)

Solver type: Linear system solver

Parameter	Value
Preordering algorithm	Nested dissection
Row preordering	On
Bunch-Kaufmann	Off
Pivoting perturbation	1.0E-8
Relative tolerance	1.0E-3
Factor in error estimate	20.0
Check tolerances	On

7.1.2. Group 2

Parameter	Value
Components	logd logk
Tolerance	1e-3

7.1.2.1. Direct (PARDISO)

Solver type: Linear system solver

Parameter	Value
Preordering algorithm	Nested dissection
Row preordering	On
Bunch-Kaufmann	Off
Pivoting perturbation	1.0E-8
Relative tolerance	1.0E-3
Factor in error estimate	20.0
Check tolerances	On

7.2. Segregated Scheme

7.2.1. Step 1

Parameter	Value
Segregated group	1
Termination technique	Iteration
Damping constant	0.5
Number of iterations	1
Maximum number of iterations	20
Tolerance	1.0E-2
Damping technique	Constant
Initial damping factor	1.0
Minimum damping factor	1.0E-4
Restriction for step size update	10.0

7.2.2. Step 2

Parameter	Value
Segregated group	2
Termination technique	Iteration
Damping constant	0.5
Number of iterations	3
Maximum number of iterations	20
Tolerance	1.0E-2
Damping technique	Constant
Initial damping factor	1.0
Minimum damping factor	1.0E-4

Restriction for step size update	10.0

7.3. Stationary

Parameter	Value
Linearity	Automatic
Maximum number of segregated iterations	100

7.4. Advanced

Parameter	Value
Constraint handling method	Elimination
Null-space function	Automatic
Automatic assembly block size	On
Assembly block size	1000
Use Hermitian transpose of constraint matrix and in symmetry detection	Off
Use complex functions with real input	Off
Stop if error due to undefined operation	On
Store solution on file	Off
Type of scaling	None
Manual scaling	
Row equilibration	On
Manual control of reassembly	Off
Load constant	On
Constraint constant	On
Mass constant	On
Damping (mass) constant	On
Jacobian constant	On

Constraint Jacobian constant	On

8. Postprocessing

9. Variables

9.1. Boundary

Name	Description	Unit	Expression
K_r_chns	Viscous force per area, r component	Pa	(eta_chns+etaT_chns) * (nr_chns * (2 * ur-2 * divU_chns/3)+nz_chns * (uz+vr))
T_r_chns	Total force per area, r component	Pa	-nr_chns * p+nr_chns * (eta_chns+etaT_chns) * (2 * ur-2 * divU_chns/3)+nz_chns * (eta_chns+etaT_chns) * (uz+vr)
K_z_chns	Viscous force per area, z component	Pa	(eta_chns+etaT_chns) * (nr_chns * (vr+uz)+nz_chns * (2 * vz-2 * divU_chns/3))
T_z_chns	Total force per area, z component	Pa	-nz_chns * p+nr_chns * (eta_chns+etaT_chns) * (vr+uz)+nz_chns * (eta_chns+etaT_chns) * (2 * vz-2 * divU_chns/3)

9.2. Subdomain

Name	Description	Unit	Expression
U_chns	Velocity field	m/s	sqrt(u^2+v^2)
V_chns	Vorticity	1/s	uz-vr
divU_chns	Divergence of velocity field	1/s	ur+vz+u/r
Dlogd_chns	Effective turbulence diffusion coefficient for logd	Pa*s	etaT_chns/sigmad_chns+eta_chns

Slogd_chns	Source term for logd	kg/(m^3*s)	Cd1_chns * (etaT_chns * exp(-logk) * pT_chns-2 * rho_chns * divU_chns/3)-Cd2_chns * rho_chns * exp(logd-nojac(logk))
d0_chns	Turbulent dissipation rate	m^2/s^3	exp(logd)
etaT_chns	Turbulent viscosity	Pa*s	nojac(rho_chns * Cmu_chns * exp(2 * logk-logd))
pT_chns	Turbulent energy production	1/s^2	2 * ur^2+2 * vz^2+(uz+vr)^2+2 * u^2/r^2-2 * divU_chns^2/3
k0_chns	Turbulent kinetic energy	m^2/s^2	exp(logk)
Dlogk_chns	Effective turbulence diffusion coefficient for logk	Pa*s	etaT_chns/sigmak_chns+eta_chns
Slogk_chns	Source term for logk	kg/(m^3*s)	etaT_chns * exp(-logk) * pT_chns-2 * rho_chns * divU_chns/3-rho_chns * exp(logd-nojac(logk))
res_logk_chns	Equation residual for logk	kg/(m^2*s)	-Dlogk_chns * (r * logkrr+r * logkzz+logkr)-r * (-rho_chns * (u * logkr+v * logkz)+Dlogk_chns * (logkr^2+logkz^2)+Slogk_chns)
res_logd_chns	Equation residual for logd	kg/(m^2*s)	-Dlogd_chns * (r * logdrr+r * logdzz+logdr)-r * (-rho_chns * (u * logdr+v * logdz)+Dlogd_chns * (logdr^2+logdz^2)+Slogd_chns)
cellRe_chns	Cell Reynolds number	1	rho_chns * U_chns * h/eta_chns
res_u_chns	Equation residual for u	Pa	r * (rho_chns * (u * ur+v * uz)+pr-F_r_chns)+2 * (eta_chns+etaT_chns) * (u/r-ur)-(eta_chns+etaT_chns) * r * (2 * urr+uzz+vrz)+2 * (eta_chns+etaT_chns) * (r * urr+r * vzr+ur-u/r)/3+2 * r * d(rho_chns * exp(logk),r)/3
res_v_chns	Equation residual for v	Pa	r * (rho_chns * (u * vr+v * vz)+pz-F_z_chns)-(eta_chns+etaT_chns) * (r * (vrr+uzr)+2 * r * vzz+uz+vr)+2 * (eta_chns+etaT_chns) * (r * urz+r *

			vzz+uz)/3+2 * r * d(rho_chns * exp(logk),z)/3
beta_r_chns	Convective field, r component	Pa*s	r * rho_chns * u
beta_z_chns	Convective field, z component	Pa*s	r * rho_chns * v
Dm_chns	Mean diffusion coefficient	kg/s	r * (eta_chns+etaT_chns)
da_chns	Total time scale factor	kg/m^2	r * rho_chns
taum_chns	GLS time-scale	m^3*s/kg	nojac(1/max(2 * rho_chns * sqrt(emetric(u,v)),48 * (eta_chns+etaT_chns)/h^2))
tauc_chns	GLS time-scale	m^2/s	0.5 * nojac(if(u^2+v^2< U_ref_chns,(u^2+v^2) *>
res_p_chns	Equation residual for p	kg/(m^2*s)	r * (rho_chns * divU_chns+d(rho_chns,r) * u+d(rho_chns,z) * v)
tau_logk_chns	GLS time-scale	m^3*s/kg	nojac(0.5 * h/max(rho_chns * U_chns,6 * Dlogk_chns/h))
tau_logd_chns	GLS time-scale	m^3*s/kg	nojac(0.5 * h/max(rho_chns * U_chns,6 * Dlogd_chns/h))